P-05-108

Forsmark site investigation

Formation factor logging in-situ by electrical methods in KFM03A and KFM04A

Martin Löfgren, Ivars Neretnieks
Department of Chemical Engineering and Technology,
Royal Institute of Technology

May 2005

Svensk Kärnbränslehantering AB
Swedish Nuclear Fuel
and Waste Management Co
Box 5864
SE-102 40 Stockholm Sweden
Tel 08-459 84 00
+46 8 459 84 00
Fax 08-661 57 19
+46 8 661 57 19

ISSN 1651-4416
SKB P-05-108

Forsmark site investigation

Formation factor logging in-situ by electrical methods in KFM03A and KFM04A

Martin Löfgren, Ivars Neretnieks
Department of Chemical Engineering and Technology,
Royal Institute of Technology

May 2005

Keywords: AP PF 400-05-038, In-situ, Formation factor, Surface conduction, Rock resistivity, Electrical conductivity.

Abstract

This report presents measurements and interpretations of the formation factor of the rock surrounding the boreholes KFM03A and KFM04A in Forsmark, Sweden. The formation factor was logged in-situ by electrical methods and is compared to formation factors obtained in the laboratory by electrical methods.

For KFM03A, the in-situ rock matrix formation factors obtained range from 2.5×10^{-5} to 5.7×10^{-4}. The in-situ fractured rock formation factors obtained range from 2.5×10^{-5} to 1.2×10^{-2}. The laboratory (rock matrix) formation factors obtained on drill core samples ranged from 4.1×10^{-5} to 9.0×10^{-4}. The formation factors appear to be fairly well log-normally distributed. The mean values and standard deviations of the obtained $\log_{10}$-normal distributions are –4.3 and 0.15, and –4.2 and 0.24 for the in-situ rock matrix and fractured rock formation factor, respectively.

For KFM04A, the in-situ rock matrix formation factors obtained range from 3.4×10^{-5} to 9.2×10^{-4}. The in-situ fractured rock formation factors obtained range from 2.9×10^{-5} to 2.8×10^{-3}. The laboratory (rock matrix) formation factors obtained on drill core samples range from 6.6×10^{-5} to 2.7×10^{-2}. The formation factors appear to be fairly well log-normally distributed. The mean values and standard deviations of the obtained $\log_{10}$-normal distributions are –4.3 and 0.16, –4.1 and 0.30, and –3.6 and 0.63 for the in-situ rock matrix and fractured rock formation factor, and laboratory formation factor, respectively.

The rock type specific formation factor distributions presented in this report suggest that the in-situ formation factor within a rock type may range over two orders of magnitude.

The results indicate relatively large differences between in-situ respectively laboratory determinations on drill cores. It may be that the rock samples taken from the drill cores and brought to the laboratory are highly altered. The alteration could either be due to de-stressing or to mechanical disturbance induced in the sample preparation. The formation factors obtained in the laboratory may be overestimated by a few factors or even as much as one order of magnitude.

Sammanfattning

Denna rapport presenterar mätningar och tolkningar av bergets formationsfaktor runt borrhålen KFM03A och KFM04A i Forsmark, Sverige. Formationsfaktorn har loggats in-situ med elektriska metoder och jämförs med formationsfaktorn erhållen i laboratoriet med elektriska metoder.

För KFM03A varierar den erhållna in-situ formationsfaktorn för bergmatrisen från $2{,}5\times10^{-5}$ till $5{,}7\times10^{-4}$. In-situ formationsfaktorn för sprickigt berg varierar från $2{,}5\times10^{-5}$ till $1{,}2\times10^{-2}$, medan den laborativa formationsfaktorn (för bergmatrisen) varierar från $4{,}1\times10^{-5}$ till $9{,}0\times10^{-4}$. Formationsfaktorn verkar vara någorlunda väl log-normalt fördelad. Medelvärdena och standardavvikelserna för de erhållna $\log_{10}$-normal fördelningarna är –4,3 och 0,15 samt –4,2 och 0,24 för in-situ formationsfaktorn för bergmatrisen respektive in-situ formationsfaktorn för sprickigt berg.

För KFM04A varierar in-situ formationsfaktorn för bergmatrisen mellan $3{,}4\times10^{-5}$ och $9{,}2\times10^{-4}$. Den erhållna in-situ formationsfaktorn för sprickigt berg varierar från $2{,}9\times10^{-5}$ till $2{,}8\times10^{-3}$, under det att den erhållna laborativa formationsfaktorn (för bergmatrisen) varierar från $6{,}6\times10^{-5}$ till $2{,}7\times10^{-2}$. Även för detta borrhål tycks formationsfaktorn vara någorlunda väl log-normalt fördelad. Medelvärdena och standardavvikelserna för $\log_{10}$-normal fördelningarna för detta borrhål är –4,3 och 0,16, –4,1 och 0,30 samt –3,6 and 0,63 för in-situ formations faktorn för bergmatrisen, in-situ formationsfaktorn för sprickigt berg, respektive den laborativa formationsfaktorn.

Resultaten som presenteras i denna rapport tyder på att formationsfaktorn inom samma bergart kan variera över två tiopotenser.

Dessutom indikerar resultaten ganska stora skillnader mellan in-situbestämningar respektive laboratoriebestämningar av formationsfaktorn. Det kan vara så att borrkärneproverna tagna från borrkärnorna till laboratoriet är betydligt störda. Störningen kan både ha sitt ursprung i avlastning och i mekanisk påverkan i samband med provförberedning. De erhållna laborativa formationsfaktorerna kan vara överskattade till det dubbla värdet eller till och med så mycket som en tiopotens.

Contents

1 Introduction

This document reports data gained from measurements of the formation factor of rock surrounding the boreholes KFM03A and KFM04A within the Forsmark site investigation area. The formation factor was logged in-situ by electrical methods. Comparisons are made with formation factors obtained in the laboratory on samples from the drill cores of KFM03A and KFM04A.

This work has been conducted according to the activity plan AP PF 400-05-038 (SKB internal controlling document). In Table 1-1 controlling documents for performing this activity are listed. The activity plan is an SKB's internal controlling document.

Other contractors performed the fieldwork and laboratory work, which is outside the framework of this activity. The interpretation of in-situ data and compilation of formation factor logs were performed by the department of Chemical Engineering and Technology at the Royal Institute of Technology in Stockholm, Sweden.

Figure 1-1 shows the Forsmark site investigation area and the location of different drill sites. KFM03A and KFM04A are located at drill sites DS3 and DS4, respectively.

Table 1-1. Controlling documents for performance of the activity.

Activity plan	**Number**	**Version**
Bestämning av formationsfaktorn från in-situ resistivitetsmätningar i KFM03A och KFM04A.	AP PF 400-05-038	1.0
Method description	**Number**	**Version**
Formation factor logging in-situ by electrical methods – Background and methodology.	SKB TR-02-27	

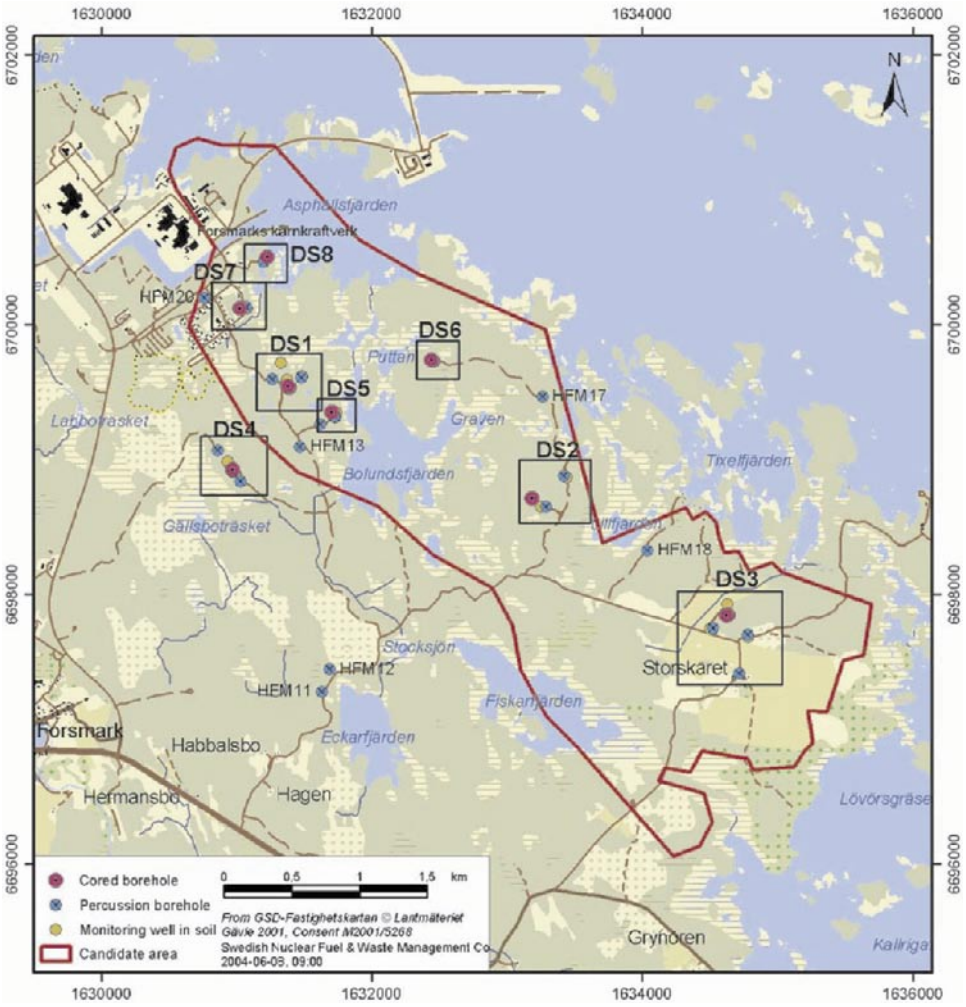

Figure 1-1. *General overview of the Forsmark site investigation area with drill sites DS1–DS8. Borehole KFM03A is situated at drill site DS3 and KFM04A at DS4.*

2 Objective and scope

The formation factor is an important parameter that may be used directly in the safety assessment. The main objective of this work is to obtain the formation factor of the rock mass surrounding the boreholes KFM03A and KFM04A. This has been achieved by performing formation factor loggings by electrical methods both in-situ and in the laboratory. The in-situ method provides a great number of formation factors obtained under more natural conditions than in the laboratory. To achieve the in-situ formation factor, results from previous loggings were used. The laboratory formation factor was obtained by performing measurements on rock samples from the drill cores of KFM03A and KFM04A.

3 Equipment

3.1 Rock resistivity measurements

The resistivity of the rock surrounding the boreholes KFM03A /1/ and KFM04A /2/ was logged in two separate campaigns using the focused rock resistivity tool Century 9072. The tool emits an alternating current perpendicular to the borehole axis from a main current electrode. The shape of the current field is controlled by electric fields emitted by guard electrodes. By using focused tools, the disturbance from the borehole is minimised. The quantitative measuring range of the Century 9072 tool is 0–50,000 ohm.m according to the manufacturer. The rock resistivity was also logged using the Century 9033 tool. However, this tool is not suitable for quantitative logging in granitic rock and the results are not used in this report.

3.2 Groundwater electrical conductivity measurements

The EC (electrical conductivity) of the borehole fluid in KFM03A /3/ and KFM04A /4/ was logged using the POSIVA difference flow meter. The tool is shown in Figure 3-1.

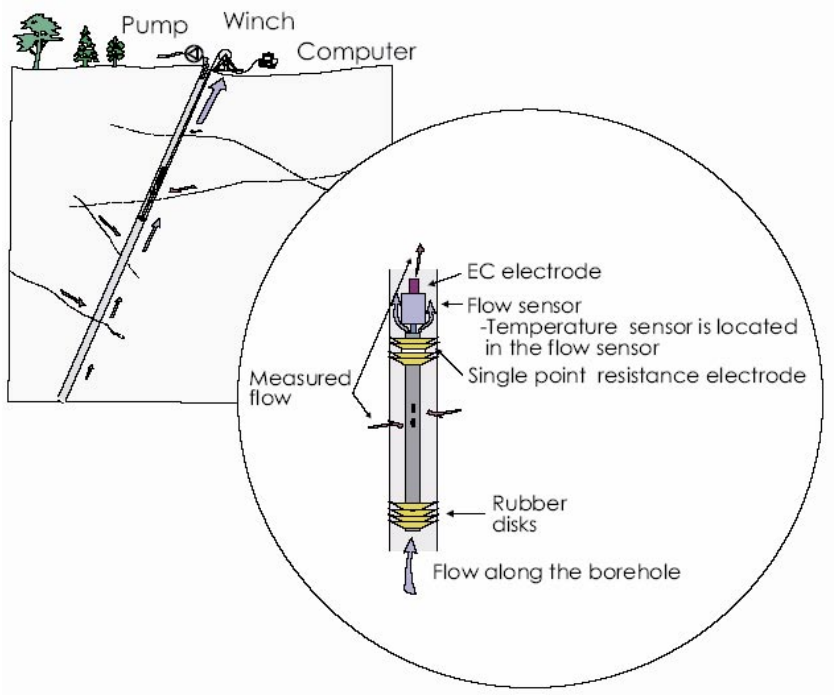

Figure 3-1. *Schematics of the POSIVA difference flow meter (image taken from /3/).*

When logging the EC of the borehole fluid, the lower rubber disks of the tool are not used. During the measurements, no drawdown is applied. Measurements were carried out before and after the difference flow logging in each borehole.

When using both the upper and the lower rubber disks, a section around a specific fracture can be packed off. By applying a drawdown at the surface, groundwater can thus be extracted from specific fractures. By also measuring the groundwater flow out of the fracture, it is calculated how long time it will take to fill up the packed off borehole section three times. During this time the EC is measured and a transient EC curve is obtained. After this time it is assumed that the measured EC is representative for the groundwater flowing out of the fracture. The measurements may be disturbed by leakage of borehole fluid into the packed off section and development of gas from species dissolved in the groundwater. Interpretations of transient EC curves are discussed in /5/. The quantitative measuring range of the EC electrode of the POSIVA difference flow meter is 0.02–11 S/m.

The EC, among other entities, of the groundwater coming from fractures in larger borehole sections is measured as a part of the hydrochemical characterisation. A section is packed off and by applying a drawdown, groundwater is extracted from fractures within the section and brought to the surface for chemical analysis. Hydrochemical characterisations of KFM03A /6/ and KFM04A /7/ were performed in two different campaigns.

3.3 Difference flow loggings

By using the POSIVA difference flow meter, water-conducting fractures can be located. The tool, shown in Figure 3-1, has a flow sensor and the flow from fractures in packed off sections can be measured. When performing these measurements, both the upper and the lower rubber disks are used. Measurements can be carried out both with and without applying a drawdown. The quantitative measuring range of the flow sensor is 0.1–5,000 ml/min.

Difference flow loggings were performed in different campaigns in KFM03A /3/ and KFM04A /4/.

3.4 Boremap loggings

The drill cores of KFM03A /8/ and KFM04A /9/ were logged together with a simultaneous study of video images of the borehole wall. This is called Boremap logging.

In the core log, fractures parting the core are recorded. Fractures parting the core that have not been induced during the drilling or core handling are called broken fractures. To decide if a fracture actually was open or sealed in the rock volume (i.e. in-situ), SKB has developed a confidence classification of open fractures expressed at three levels, “possible”, “probable” and “certain”, based on the aperture, weathering and fit of the fracture /8/.

Out of the 722 broken fractures that were interpreted as sealed in-situ in the core logging of KFM03A, only 9 had the confidence “certain”. For KFM04A, 1,968 fractures were classified as broken (including the broken fractures of the upper 100 m of the drill core). Out of these, 742 fractures were classified as sealed but only 176 with certainty. Hence, there is a strong uncertainty whether broken fractures were open before drilling or during/after drilling /10/. For this reason, it was decided to treat all broken fractures as potentially open in-situ in this work.

In previous reports dealing with formation factor logging in-situ by electrical methods in Forsmark /11/ and Simpevarp /5/, an old nomenclature for the Boremap logging was used. In the old nomenclature, broken fractures were called natural fractures. In /5/ and /11/ it was assumed that all natural fractures were potentially open in-situ. As it is assumed that all broken fractures are potentially open in-situ in this report, the methodology used does not differ from that used in /5/ and /11/.

In the Boremap logging, parts of the core that are crushed or lost are also recorded, as well as the spatial distribution of different rock types.

4 Execution

4.1 Theory

4.1.1 The formation factor

The theory applied for obtaining formation factors by electrical methods is described in /12/. The formation factor is the ratio between the diffusivity of the rock matrix to that of free pore water. If the species diffusing through the porous system is much smaller than the characteristic length of the pores and no interactions occur between the mineral surfaces and the species, the formation factor is only a geometrical factor that is defined by the transport porosity, the tortuosity and the constrictivity of the porous system:

$$F_f = \frac{D_e}{D_w} = \varepsilon_t \frac{\delta}{\tau^2} \qquad 4\text{-}1$$

where F_f (–) is the formation factor, D_e (m^2/s) is the effective diffusivity of the rock, D_w (m^2/s) is the diffusivity in the free pore water, ε_t (–) is the transport porosity, τ (–) is the tortuosity, and δ (–) is the constrictivity. When obtaining the formation factor with electrical methods, the Einstein relation between diffusivity and ionic mobility is used:

$$D = \frac{\mu RT}{zF} \qquad 4\text{-}2$$

where D (m^2/s) is the diffusivity, μ ($m^2/V\times s$) is the ionic mobility, z (–) the charge number and R (J/mol×K), T (K) and F (C/mol), are the gas constant, temperature, and Faraday constant respectively. From the Einstein relation it is easy to show that the formation factor also is given by the ratio of the pore water resistivity to the resistivity of the saturated rock /13/:

$$F_f = \frac{\rho_w}{\rho_r} \qquad 4\text{-}3$$

where ρ_w (ohm.m) is the pore water resistivity and ρ_r (ohm.m) is the rock resistivity. The resistivity of the saturated rock can easily be obtained by standard geophysical methods.

At present it is not feasible to extract pore water from the rock matrix in-situ. Therefore, it is assumed that the pore water is in equilibrium with the free water surrounding the rock, and measurements are performed on this free water. The validity of this assumption has to be discussed for every specific site.

The resistivity is the reciprocal to electrical conductivity. Traditionally the EC (electrical conductivity) is used when measuring on water and resistivity is used when measuring on rock.

4.1.2 Surface conductivity

In intrusive igneous rock the mineral surfaces are normally negatively charged. As the negative charge often is greater than what can be balanced by cations specifically adsorbed on the mineral surfaces, an electrical double layer with an excess of mobile cations will form at the pore wall. If a potential gradient is placed over the rock, the excess cations in the electrical double layer will move. This process is called surface conduction and this additional conduction may have to be accounted for when obtaining the formation factor of rock saturated with a pore water of low ionic strength. If the EC of the pore water is around 0.5 S/m or above, errors associated with surface conduction are deemed to be acceptable.

This criterion is based on laboratory work by /14/ and /13/. The effect of the surface conduction on rock with formation factors below 1×10^{-5} was not investigated in these works. In this report surface conduction has not been accounted for, as only the groundwater in the upper 100 or 200 m of the boreholes has a low ionic strength and as more knowledge is needed on surface conduction before performing corrections.

4.1.3 Artefacts

Comparative studies have been performed on a large number of 1–2 cm long samples from Äspö in Sweden /14/. Formation factors obtained with an electrical resistivity method using alternating current were compared to those obtained by a traditional through diffusion method, using uranine as the tracer. The results show that formation factors obtained by the electrical resistivity measurements are a factor of about 2 times larger that those obtained by through diffusion measurements. A similar effect was found on granitic samples up to 12 cm long, using iodide in tracer experiments /15/. The deviation of a factor 2 between the methods may be explained by anion exclusion of the anionic tracers. Previously performed work suggests that the Nernst-Einstein equation between the diffusivity and electrical conductivity is generally applicable in granitic rock and that no artefacts give rise to major errors. It is uncertain, however, to what extent anion exclusion is related to the degree of compression of the porous system in-situ due to the overburden.

4.1.4 Fractures in-situ

In-situ rock resistivity measurements are highly disturbed by free water in open fractures. The current sent out from the downhole tool in front of an open fracture will be propagated both in the porous system of the rock matrix and in the free water in the open fracture. Due to the low formation factor of the rock matrix, current may be preferentially propagated in a fracture intersecting the borehole if its aperture is on the order of 10^{-5} m or more.

There could be some confusion concerning the terminology of fractures. In order to avoid confusion, an organization sketch of different types of fractures is shown in Figure 4-1. The subgroups of fractures that interfere with the rock resistivity measurements are marked with grey.

The information concerning different types of fractures in-situ is obtained from the interpretation of the Boremap logging and in the hydraulic flow logging. A fracture intersecting the borehole is most likely to part the drill core. In the core log, fractures that part the core are either broken or operational (drill-induced). Unbroken fractures, which

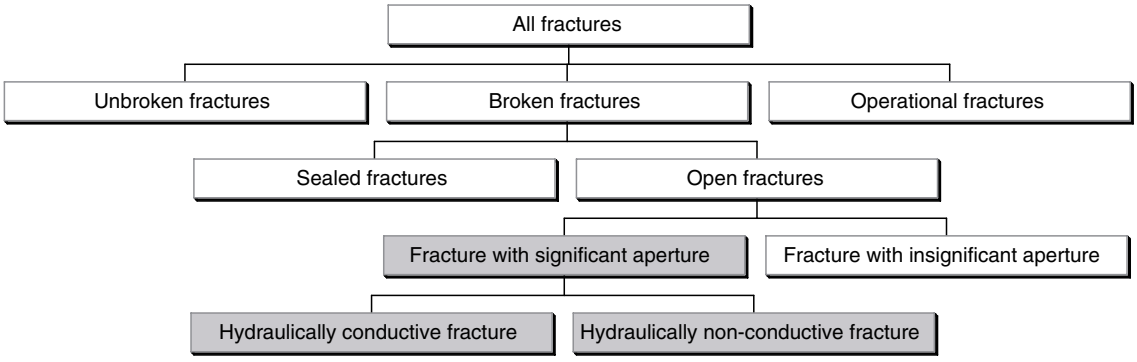

Figure 4-1. *Organization sketch of different types of fractures in-situ.*

do not part the core, are sealed or only partly open. Laboratory results suggest that sealed fractures generally have no major interference on rock resistivity measurements. The water-filled void in partly open fractures can be included in the porosity of the rock matrix.

Broken fractures are either interpreted as open or sealed. Open fractures may have a significant or insignificant aperture. With insignificant aperture means an aperture so small that the amount of water held by the fracture is comparable with that held in the adjacent porous system. In this case the "adjacent porous system" is the porous system of the rock matrix the first few centimetres from the fracture.

If the fracture has a significant aperture, it holds enough water to interfere with the rock resistivity measurements. Fractures with a significant aperture may be hydraulically conductive or non-conductive, depending on how they are connected to the fracture network and on the hydraulic gradients of the system.

Due to uncertainties in the interpretation of the core logging, all broken fractures are assumed to potentially have a significant aperture.

4.1.5 Rock matrix and fractured rock formation factor

In this report the rock resistivity is used to obtain formation factors of the rock surrounding the borehole. The obtained formation factors may later be used in models for radionuclide transport in fractured crystalline rock. Different conceptual approaches may be used in the models. Therefore this report aims to deliver formation factors that are defined in two different ways. The first is the "rock matrix formation factor", denoted by F_f^{rm} (–). This formation factor is representative for the solid rock matrix, as the traditional formation factor. The other one is the "fractured rock formation factor", denoted by F_f^{fr} (–), which represents the diffusive properties of a larger rock mass, where fractures and voids holding stagnant water are included in the porous system of the rock matrix. Further information on the definition of the two formation factors could be found in /5/.

The rock matrix formation factor is obtained from rock matrix resistivity data. When obtaining the rock matrix resistivity log from the in-situ measurements, all resistivity data that may have been affected by open fractures have to be sorted out. With present methods one cannot with certainty separate open fractures with a significant aperture from open fractures with an insignificant aperture in the interpretation of the core logging. It should be mentioned that there is an attempt to assess the fracture aperture in the interpretation of the core logging. However, this is done on a millimetre scale. Fractures may be significant even if they only have apertures some tens of micrometres.

By investigating the rock resistivity log at a fracture, one could draw conclusions concerning the fracture aperture. However, for formation factor logging by electrical methods this is not an independent method and cannot be used. Therefore, all broken fractures have to be considered as potentially open and all resistivities obtained close to a broken fracture detected in the core logging are sorted out. By examining the resistivity logs obtained by the Century 9072 tool, it has been found that resistivity values obtained within 0.5 m from a broken fracture generally should be sorted out. This distance includes a safety margin of 0.1–0.2 m.

The fractured rock formation factor is obtained from fractured rock resistivity data. When obtaining the fractured rock resistivity log from the in-situ measurements, all resistivity data that may have been affected by free water in hydraulically conductive fractures, detected in the in-situ flow logging, have to be sorted out. By examining the resistivity logs obtained by

the Century 9072 tool, it has been found that resistivity values obtained within 0.5 m from a hydraulically conductive fracture generally should be sorted out. This distance includes a safety margin of 0.1–0.2 m.

4.2 Rock resistivity measurements in-situ

4.2.1 Rock resistivity log KFM03A

The rock resistivity of KFM03A was logged on the 11th of August 2003 (activity id 12975941) /1/. The in-situ rock resistivity was obtained using the focused rock resistivity tool Century 9072. The borehole was logged between 3–1,000 m. In order to obtain an exact depth calibration, the track marks made in the borehole were used. According to /1/ an exact depth calibration was not obtained. The following deviations in the calibration with depth are reported.

The deviation is fairly linear with the borehole length. The borehole length reported in /1/ was corrected between 110–1,000 m by subtracting the deviation obtained by the linear equation shown in Figure 4-2.

In Figure 4-2 the borehole length is according to the reference marks. No correction in reported borehole length was made between 0–110 m.

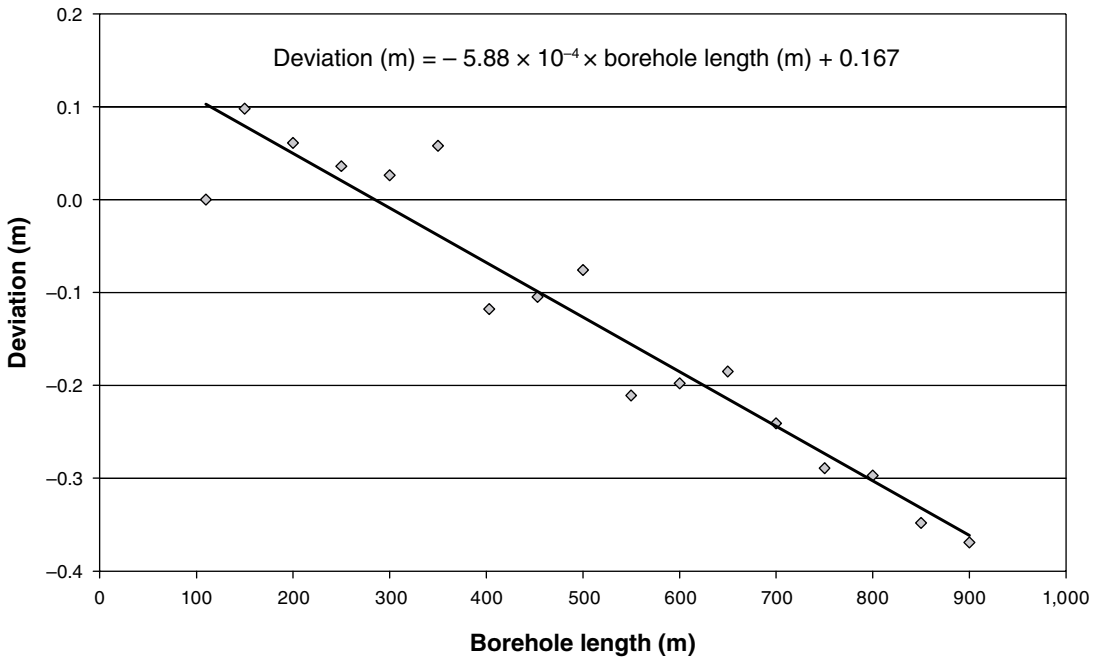

Figure 4-2. *Deviations in borehole length in KFM03A.*

Table 4-1. Deviation in borehole lengths. Data from /1/.

Reference mark (m)	110	150	200	250	300	350	403	453	500
Deviation (m)	0	0.098	0.061	0.036	0.026	0.058	–0.12	–0.11	–0.076
Reference mark (m)	550	600	650	700	750	800	850	900	
Deviation (m)	–0.21	–0.20	–0.19	–0.24	–0.29	–0.30	–0.35	–0.37	

4.2.2 Rock matrix resistivity log KFM03A

After adjusting the borehole length of the in-situ rock resistivity log, all resistivity data obtained within 0.5 m from a broken fracture detected in the core log were sorted out. In the core log (activity id 13029964), a total of 994 broken fractures are recorded between 102.2–1,000.1 m. Three crush zones and three zones where the core has been lost are recorded. A total of 1.15 m of the core was crushed or lost. Broken fractures can potentially intersect the borehole in zones where the core is crushed or lost. Therefore, a broken fracture was assumed every decimetre in these zones. The locations of broken fractures in KFM03A are shown in Appendix B1. A total of 4,532 rock matrix resistivities were obtained between 102–1,000 m. 3,773 (83%) of the rock matrix resistivities were within the quantitative measuring range of the Century 9072 tool. The rock matrix resistivity log between 102–1,000 m is shown in Appendix B1.

Figure 4-3 shows the distribution of the rock matrix resistivities obtained between 102–1,000 m in KFM03A. The histogram ranges from 0–100,000 ohm.m and is divided into sections of 5,000 ohm.m.

4.2.3 Fractured rock resistivity log KFM03A

After adjusting the borehole length of the in-situ rock resistivity log, all resistivity data obtained within 0.5 m from a hydraulically conductive fracture, detected in the difference flow logging /3/, were sorted out. For the difference flow log, no correction in the reported borehole length was needed. A total of 52 hydraulically conductive fractures were detected in KFM03A. The locations of hydraulically conductive fractures in KFM03A are shown in Appendix B1. A total of 8,504 fractured rock resistivities were obtained between 102–1,000 m. 7,228 (85%) of the fractured rock resistivities were within the quantitative measuring range of the Century 9072 tool. The fractured rock resistivity log between 102–1,000 m is shown in Appendix B1.

Figure 4-4 shows a histogram of the fractured rock resistivities obtained between 102–1,000 m in KFM03A. The histogram ranges from 0–100,000 ohm.m and is divided into sections of 5,000 ohm.m.

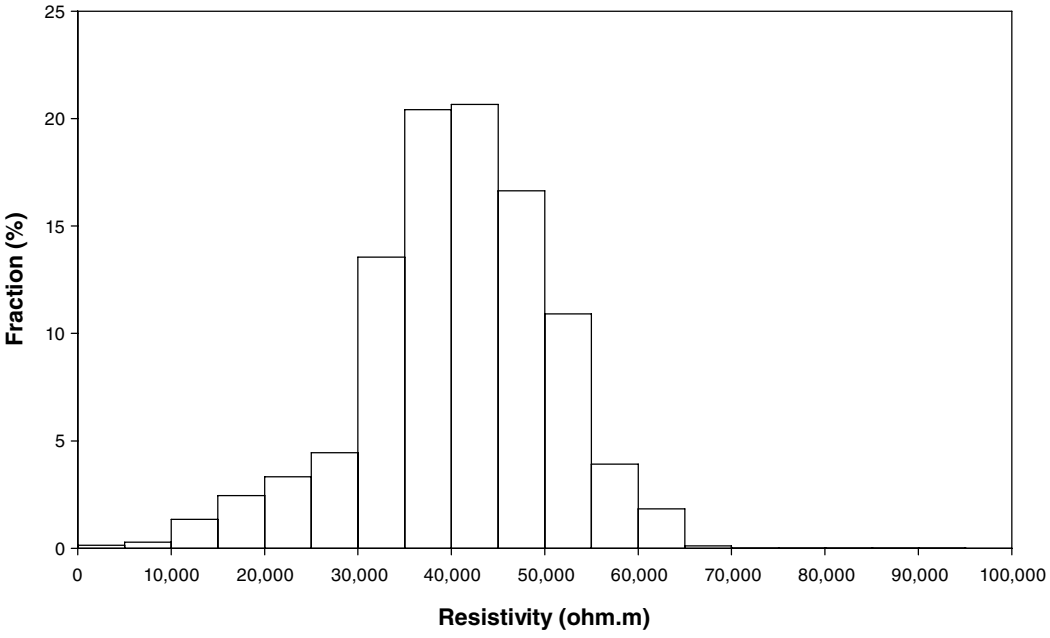

Figure 4-3. *Distribution of rock matrix resistivities in KFM03A.*

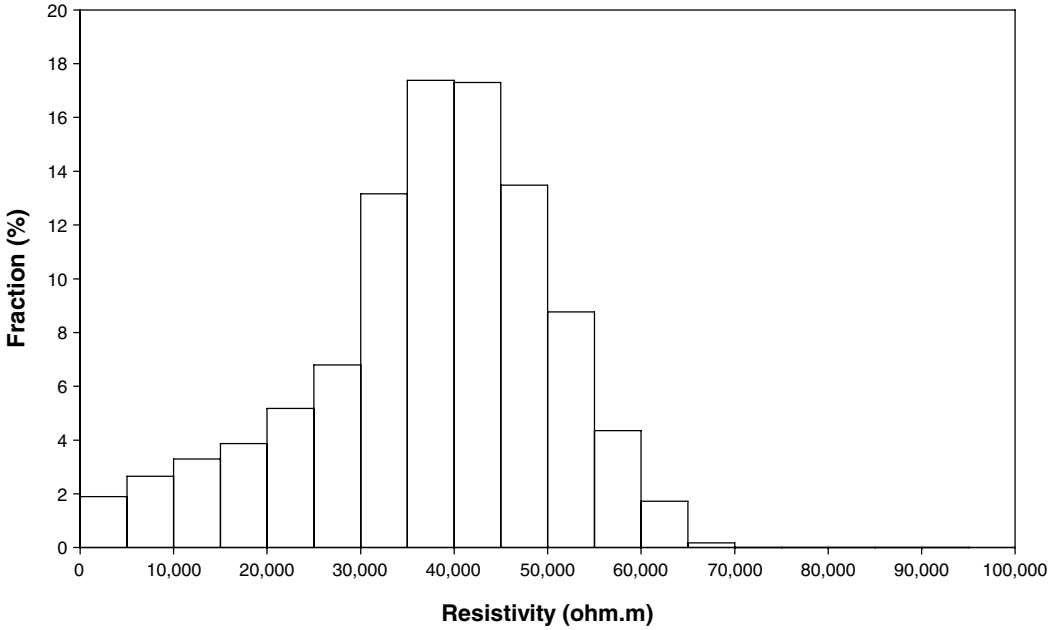

Figure 4-4. *Histogram of fractured rock resistivities in KFM03A.*

4.2.4 Rock resistivity KFM04A

The rock resistivity of KFM04A was logged on the 23rd of November 2003 (activity id 13016717) /2/. The in-situ rock resistivity was obtained using the focused Century 9072 tool. The borehole was logged between 110.0–998.5 m. In order to obtain an exact depth calibration, the track marks made in the borehole were used. According to /2/ an exact depth calibration was not obtained. The following deviations in the calibration with depth are reported.

The deviation is fairly linear with the borehole length. The borehole length reported in /2/ was corrected between 119–998.5 m by subtracting the deviations obtained by the linear equation shown in Figure 4-5.

In Figure 4-5 the borehole length is according to the reference marks. No correction in reported borehole length was made between 0–119 m.

4.2.5 Rock matrix resistivity log KFM04A

After adjusting the borehole length of the in-situ rock resistivity log, all resistivity data obtained within 0.5 m from a broken fracture, detected in the core log, were sorted out. In the core log (activity id 13015663), a total of 1,873 broken fractures are recorded between 108.6–999.8 m. In addition two crush zones but no zones where the core is lost are recorded. A total of 0.29 m of the core is crushed. Broken fractures can potentially intersect the borehole in zones where the core is crushed or lost. Therefore, a broken fracture was assumed every decimetre in these zones. The locations of broken fractures in KFM04A are shown in Appendix B2. A total of 3,081 rock matrix resistivities were obtained between 110–999 m. All values were within the quantitative measuring range of the Century 9072 tool. The rock matrix resistivity log between 110–999 m is shown in Appendix B2.

Figure 4-6 shows a histogram of the rock matrix resistivities obtained between 110–999 m in KFM04A. The histogram ranges from 0–100,000 ohm.m and is divided into sections of 5,000 ohm.m.

Table 4-2. Deviation in borehole lengths. Data from /2/.

Reference mark (m)	119	150	200	250	300	350	400	450	500
Deviation (m)	0	0.04	0.08	0.04	0.12	0.18	0.25	0.27	0.32
Reference mark (m)	550	600	650	700	750	800	850	900	950
Deviation (m)	0.41	0.44	0.47	0.59	0.63	0.77	0.85	0.79	0.96

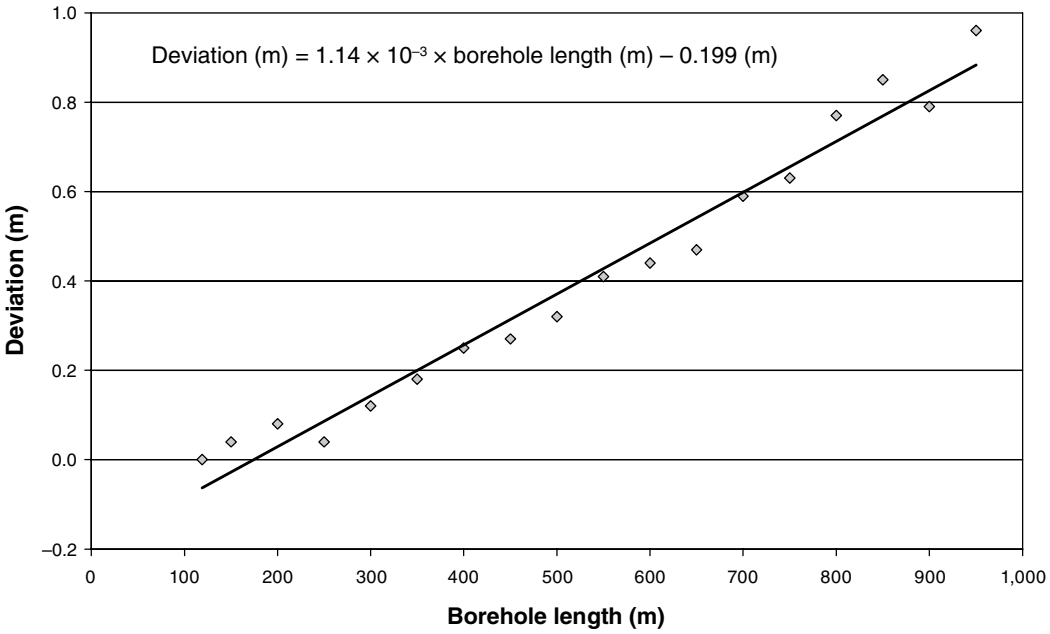

Figure 4-5. *Deviations in borehole length in KFM04A.*

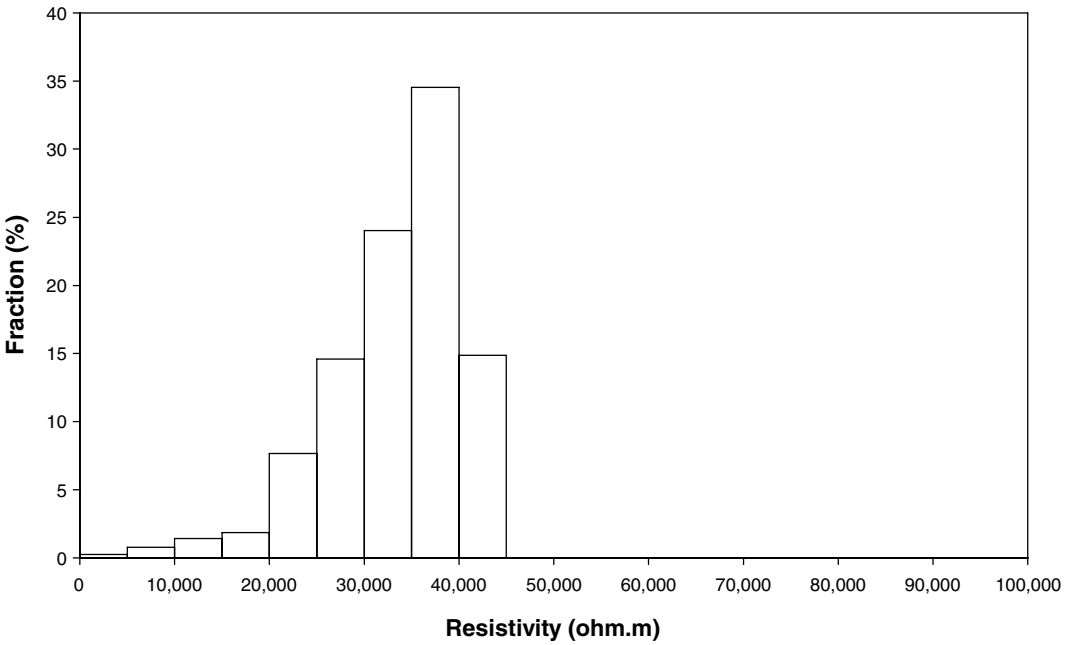

Figure 4-6. *Histogram of rock matrix resistivities in KFM04A.*

From the shape of the histogram in Figure 4-6, one may suspect that the upper quantitative response limit of the Century 9072 tool was lower than 50,000 ohm.m when measuring in KFM04A. The highest rock resistivity obtained in KFM04A was 44,565 ohm.m.

4.2.6 Fractured rock resistivity log KFM04A

After adjusting the borehole length of the in-situ rock resistivity log, all resistivity data obtained within 0.5 m from a hydraulically conductive fracture, detected in the difference flow logging /4/, were sorted out. For the difference flow log, no correction in the reported borehole length was needed. A total of 71 hydraulically conductive fractures were detected in KFM04A. The locations of hydraulically conductive fractures in KFM04A are shown in Appendix B2. A total of 8,263 fractured rock resistivities were obtained between 110–999 m. All values were within the quantitative measuring range of the Century 9072 tool. The fractured rock resistivity log between 110–999 m is shown in Appendix B2.

Figure 4-7 shows a histogram of the fractured rock resistivities obtained between 110–999 m in KFM04A. The histogram ranges from 0–100,000 ohm.m and is divided into sections of 5,000 ohm.m.

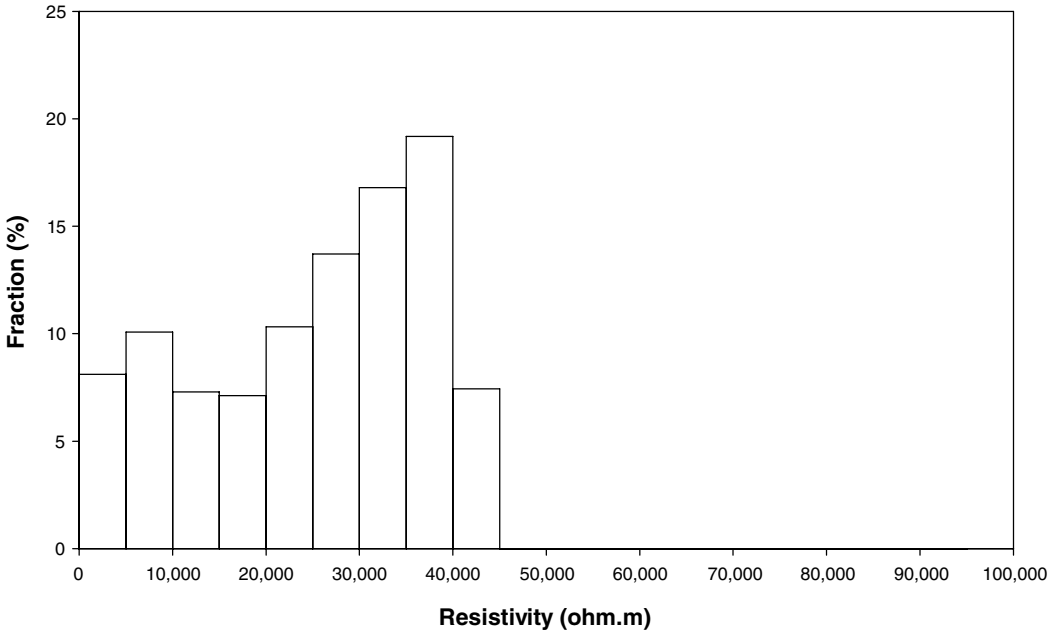

Figure 4-7. *Histogram of fractured rock resistivities in KFM04A.*

4.3 Groundwater EC measurements in-situ

4.3.1 General comments

Some of the electrical conductivities presented in this section have been corrected for the temperature to conductivities at 25°C. Other electrical conductivities are uncorrected. The corrected value should be used for in-situ evaluations. However, as the corrections are insignificant (only a few percent) in comparison to other uncertainties, both corrected and uncorrected values have been used.

4.3.2 EC measurements in KFM03A

EC of the borehole fluid in KFM03A was measured before and after two different difference flow logging campaigns on four occasions shown in Table 4-3 /3/.

EC of groundwater extracted from a number of specific fractures between 388–986 m was measured in two different campaigns using the POSIVA difference flow meter /3/. The first campaign was carried out between 2003-08-21 and 2003-08-25 and the second campaign between 2004-05-06 and 2004-05-08. The resulting fracture specific ECs are shown in Table 4-4.

EC was also measured on groundwater extracted from a number of packed off sections in KFM03A in the hydrochemical characterisation /6/ which was carried out between 2003-09-11 and 2004-04-27. The resulting fracture specific ECs are displayed in Table 4-4.

The borehole fluid EC logs obtained in KFM03A are presented in Figure 4-8, together with the fractures specific ECs shown in Table 4-4. If there was more than one fracture in a packed off section, the mean value of the borehole lengths of the fractures is used. The numbers associated with the borehole fluid EC logs in Figure 4-8 are according to Table 4-3.

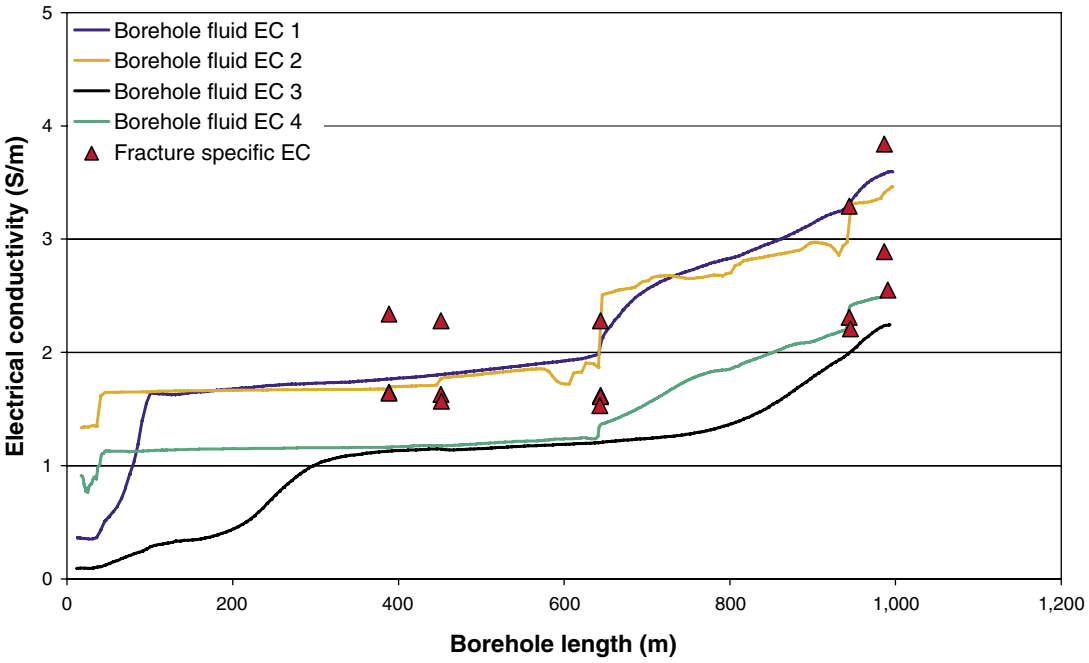

Figure 4-8. *Groundwater EC in KFM03A.*

Table 4-3. Measurements of borehole fluid EC, KFM03A.

Measurement	Activity id	Start date
Before first difference flow logging (1)	12980490	2003-08-14
After first difference flow logging (2)	12980502	2003-08-25
Before second difference flow logging (3)	13015140	2004-05-05
After second difference flow logging (4)	13015142	2004-05-08

Table 4-4. Fracture specific ECs, KFM03A.

Measurement	Borehole section (m)	Location of fractures (m)	EC (S/m)
Difference flow, campaign 1	388.2–389.2	388.6	2.34
Difference flow, campaign 2	388.0–389.0	388.6	1.65
Hydrochemical characterisation	386.0–391.0	388.6	1.64
Difference flow, campaign 1	450.9–451.9	451.3	2.28
Difference flow, campaign 2	450.8–451.8	451.3	1.63
Hydrochemical characterisation	448.5–455.6	449.4, 451.3, 454.8	1.57
Difference flow, campaign 1	643.5–644.5	643.9	2.28
Difference flow, campaign 2	643.4–644.4	643.9	1.62 1.61*
Hydrochemical characterisation	639.0–646.1	642.2, 643.9	1.53
Difference flow, campaign 1	943.9–944.9	944.2	3.29
Difference flow, campaign 2	943.7–944.7	944.2	2.31
Hydrochemical characterisation	939.5–946.6	944.2, 946.5	2.21
Difference flow, campaign 1	985.9–986.9	986.2, 986.5	3.84
Difference flow, campaign 2	985.9–986.9	986.2, 986.5	2.89
Hydrochemical characterisation	980.0–1,001.2	986.2, 986.5, 992.9, 993.8, 994.0	2.55

* EC measurement repeated.

4.3.3 EC measurements in KFM04A

EC of the borehole fluid in KFM04A was measured before and after a difference flow logging campaign on two different occasions shown in Table 4-5 /4/.

EC of groundwater extracted from a number of specific fractures between 118–360 m was measured in a campaign using the POSIVA difference flow meter /4/. The campaign was carried out between 2004-03-21 and 2004-03-27. The resulting fracture specific ECs are presented in Table 4-6.

EC was also measured on groundwater extracted from two packed off sections of KFM04A in the hydrochemical characterisation /7/ which was performed between 2004-01-09 and 2004-05-11. The resulting fracture specific ECs are shown in Table 4-6.

The borehole fluid EC logs obtained in KFM04A are given in Figure 4-9, together with the fractures specific ECs displayed in Table 4-6. If a packed off section included more than one fracture, the mean value of the borehole lengths of the fractures is used. The numbers associated with the borehole fluid EC logs in Figure 4-9 are according to Table 4-5.

Table 4-5. Measurements of borehole fluid EC, KFM04A.

Measurement	Activity id	Start date
Before difference flow logging (1)	13010318	2004-03-10
After difference flow logging (2)	13010388	2004-03-26

Table 4-6. Fracture specific ECs, KFM04A.

Measurement	Borehole section (m)	Location of fractures (m)	EC (S/m)
Difference flow	115.69–116.69	116.3	0.87
Difference flow	206.55–207.55	207.1	1.40
Difference flow	234.99–235.99	235.6	1.46
Hydrochemical characterisation	230.5–237.6	232.7, 234.0, 235.6	1.68
Difference flow	296.46–297.46	297.1	1.48
Difference flow	359.21–360.21	359.8	1.45
Hydrochemical characterisation	354.0–361.1	355.5, 357.8, 358.2, 359.8	1.63

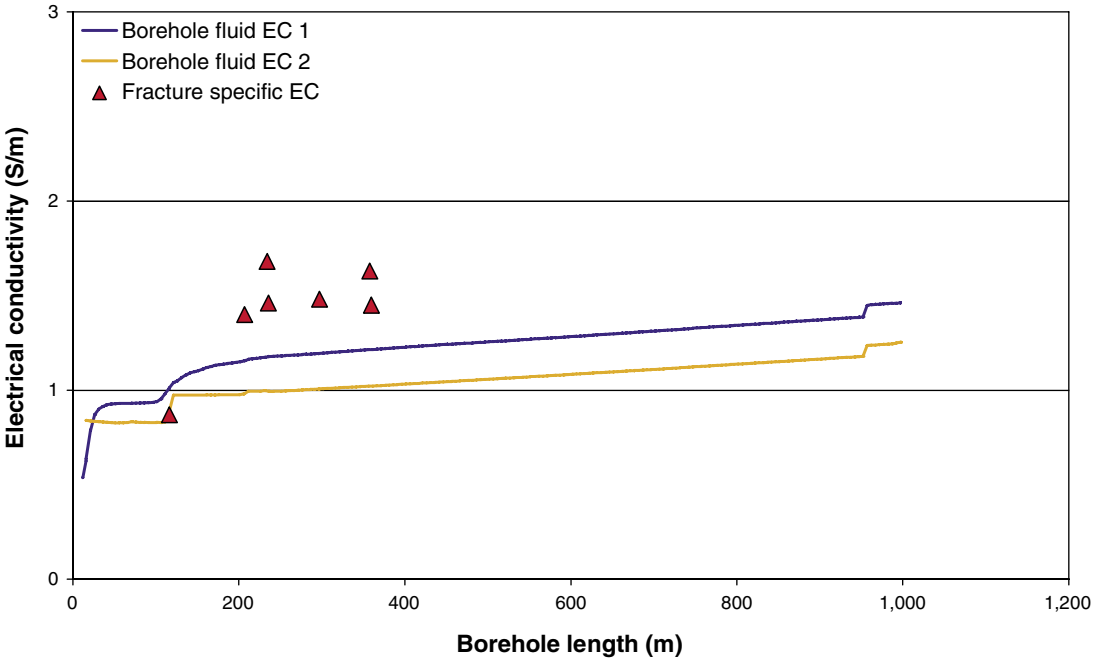

Figure 4-9. Groundwater EC in KFM04A.

4.3.4 EC measurements in KFM01A–KFM05A

As groundwater ECs were only obtained in the lower part of KFM03A and in the upper part of KFM04A, extrapolations have to be made for the intermediate interval. It is preferable to avoid such extrapolations, which may be quite uncertain, by obtaining in-situ data distributed over the entire borehole length. In this case this was not feasible. It was decided to base the extrapolations not only on the data obtained in KFM03A and KFM04A, but also on the data obtained in KFM01A, KFM02A, and KFM05A, which are boreholes within the Forsmark candidate area, see Figure 1-1. Figure 4-10 shows the fracture specific

groundwater ECs obtained in difference flow loggings or in hydrochemical characterisations in the boreholes KFM01A–KFM05A. As the boreholes have different inclinations (shown in Table 4-7), this was corrected for and the x-axis in Figure 4-10 represents the vertical borehole depth.

Different altitudes of the drilling sites (which are in the range of a few metres) were not corrected for. Table 4-7 shows the ECs used from KFM01A, KFM02A, and KFM05A and whether the values were obtained by difference flow logging (Diff) or by hydrochemical characterisation (HC).

In the hydrogeochemical evaluation of the Forsmark site /20/ it is suggested that there is a transition from fresh-meteoric waters to brackish-marine waters in the upper 200 m of the bedrock. It is also suggested that there may be a transition towards ancient brine groundwater below 800 m. This is reflected in the data in Figure 4-10. What is interesting to note is that below the vertical borehole depth 200 m, the ratio of the highest to the lowest groundwater EC shown in Figure 4-10 is only 2.7. As the groundwater EC data follow a somewhat predictable profile, where the shattering is less than the range, the errors arising from the extrapolation is likely to be smaller than a factor of 2.7. It should be kept in mind that the variation in groundwater EC at depth is small compared to the variation found in the rock resistivity measurements.

Great care should be taken when making extrapolations in the zone where the transition from fresh-meteoric waters to brackish-marine waters takes place. The ratio of the highest to the lowest groundwater EC shown in Figure 4-10, which was obtained above the vertical borehole depth 200 m, is as much as 13. Furthermore, surface conduction greatly disturbs formation factor measurements by electrical methods in groundwater with a low salinity. Therefore, the method may not be applicable in the transition zone from fresh-meteoric waters to brackish-marine waters.

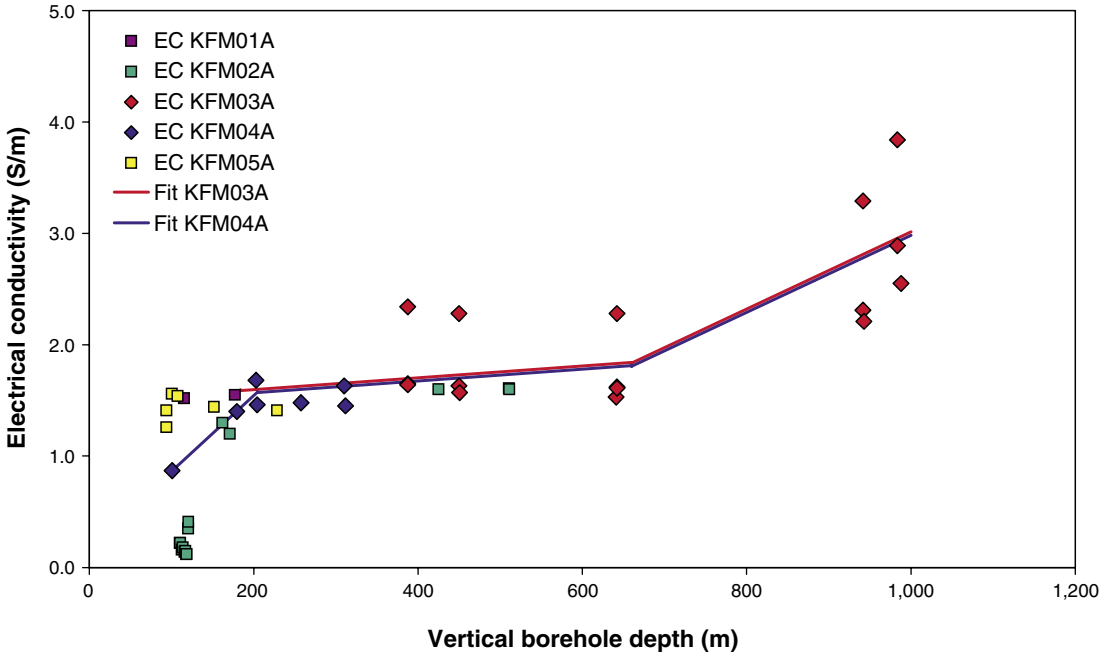

Figure 4-10. *Groundwater EC in KFM01A–KFM05A.*

Table 4-7. ECs in KFM01A, KFM02A, and KFM05A.

Borehole	Inclination	Borehole length	Borehole depth	EC	Method
KFM01A	84.7°	116.0	115.5	1.52	HC /16/
KFM01A		178.0	177.2	1.55	HC
KFM02A	84.7°	110.7	110.2	0.22	Diff /17/
KFM02A		111.1	110.6	0.22	Diff
KFM02A		112.9	112.4	0.16	Diff
KFM02A		114.2	113.7	0.18	Diff
KFM02A		116.6	116.1	0.14	Diff
KFM02A		117.5	117.0	0.15	Diff
KFM02A		118.3	117.8	0.12	Diff
KFM02A		119.0	118.5	0.12	Diff
KFM02A		120.9	120.4	0.35	Diff
KFM02A		121.1	120.5	0.41	Diff
KFM02A		162.8	162.1	1.3	Diff
KFM02A		171.7	171.0	1.2	Diff
KFM02A		426.8	425.0	1.6	Diff
KFM02A		513.0	510.8	1.61	HC /18/
KFM02A		513.6	511.4	1.6	Diff
KFM03A	85.8°				
KFM04A	60.1°				
KFM05A	59.8°	108.9	94.1	1.41	Diff /19/
KFM05A		108.9	94.1	1.26	Diff
KFM05A		116.5	100.7	1.56	Diff
KFM05A		124.3	107.4	1.54	Diff
KFM05A		175.6	151.8	1.44	Diff
KFM05A		264.4	228.5	1.41	Diff

4.3.5 EC extrapolations in KFM03A and KFM04A

In KFM03A, the transition from fresh-meteoric waters to brackish-marine waters is not characterised at all by the obtained fracture specific ECs. Therefore, it was decided not to extrapolate the EC profile in the shallower 200 m of the borehole. Below 200 m, the assumed EC profile is based on ECs from KFM02A–KFM05A. The solid red line in Figure 4-10 shows the assumed EC profile in KFM03A. The equations for the two straight lines, converted to borehole lengths, are:

Borehole length 200–663 m, KFM03A:

$$EC\ (S/m) = 5.33 \times 10^{-4} \times \text{borehole lenght (m)} + 1.47 \qquad 4\text{-}4$$

Borehole length 663–1,000 m, KFM03A:

$$EC\ (S/m) = 3.47 \times 10^{-3} \times \text{borehole length (m)} - 0.479 \qquad 4\text{-}5$$

In KFM04A, most of the transition from fresh-meteoric waters to brackish-marine waters appears to have taken place above the borehole length 116 m, where the first groundwater EC was obtained in the difference flow logging. As it is unknown at what exact depth the transition takes place, it is recommended not to extrapolate the groundwater EC profile

to shallower depths. As no fracture specific EC values were obtained below the borehole length 360 m, the extrapolated EC profile below this depth is based on ECs from KFM02A and KFM03A. The solid blue line in Figure 4-10 shows the assumed EC profile in KFM04A. The equations for the three straight lines, converted to borehole lengths, are:

KFM04A: Borehole length 110–205 m:

$$EC\ (S/m) = 5.88 \times 10^{-3} \times \text{borehole length (m)} + 0.161 \qquad 4\text{-}6$$

KFM04A: Borehole length 205–663 m:

$$EC\ (S/m) = 4.61 \times 10^{-4} \times \text{borehole length (m)} + 1.27 \qquad 4\text{-}7$$

KFM04A: Borehole length 663–1,000 m:

$$EC\ (S/m) = 3.00 \times 10^{-3} \times \text{borehole length (m)} - 0.414 \qquad 4\text{-}8$$

4.3.6 Electrical conductivity of the pore water

The rock surrounding KFM03A and KFM04A has a relatively low fracture frequency. In KFM03A, on average 1.1 broken fractures per metre part the drill core. From the rock resistivity log one can see that a substantial fraction of the broken fractures are open with a significant aperture. By using the POSIVA difference flow meter, groundwater could be withdrawn from most part of the borehole. By visual inspection of the rock resistivity logs, shown in Appendix B1, one can see that the typical block of solid rock between open fractures with significant apertures is a few metres wide. Even the centre of such a block would be fairly well equilibrated with non-sorbing solutes in a 1,000 years perspective. There are a few sections of KFM03A that are more sparsely fractured where it may be speculative to claim that the rock matrix is equilibrated with freely flowing groundwater at the corresponding depth. However, in general it seems reasonable to say that the pore water of the rock matrix is fairly well equilibrated with the freely flowing groundwater at the corresponding depth.

In KFM04A, on average 2.1 broken fractures per metre part the drill core. The upper 500 m of KFM04A is very fractured while the lower part is more sparsely fractured (Appendix B2). By investigating the rock resistivity log it seems reasonable to assume that most of the pore water of the rock matrix is fairly well equilibrated with the freely flowing groundwater at the corresponding depth, even in the lower part of the borehole. However, as groundwater in general could not be withdrawn by the POSIVA difference flow meter and no fracture specific ECs could be obtained in the lower part of the borehole, the assumed pore water EC profile of KFM04A is somewhat speculative.

It is subjectively assessed that the errors, arising from the lack of knowledge in groundwater and pore water ECs, on average should not be more than a factor of 3.

4.4 Formation factor measurements in the laboratory

The laboratory work was performed by Geovista AB. Formation factors were obtained on 5 and 17 rock samples taken from the drill core of KFM03A and KFM04A respectively. The sample length was, in general, 3 cm. The obtained formation factors are tabulated in Appendix A1 and A2.

5 Results

5.1 Laboratory formation factor

The formation factors obtained in the laboratory are tabulated in Appendix A1 and A2 for KFM03A and KFM04A, respectively. As only 5 samples from the drill core of KFM03A were measured on, no statistical treatment of the results has been made.

The 17 laboratory formation factors obtained in KFM04A were treated statistically. By using the normal-score method, as described in /21/, to determine the likelihood that a set of data is normally distributed, the mean value and standard deviation of the logarithm ($\log_{10}$) of the formation factors could be determined. Figure 5-1 shows the distribution of the laboratory formation factors obtained in KFM04A.

As can be seen in Figure 5-1, the obtained formation factors range over three orders of magnitude and deviates somewhat from the log-normal distribution. However, it should be kept in mind that only a few data points were used. The mean value and standard deviation of the distribution in Figure 5-1 are shown in Table 5-2. The laboratory formation factor logs of KFM03A and KFM04A are presented in Appendix C1 and C2 respectively, as compared to the in-situ formation factor logs.

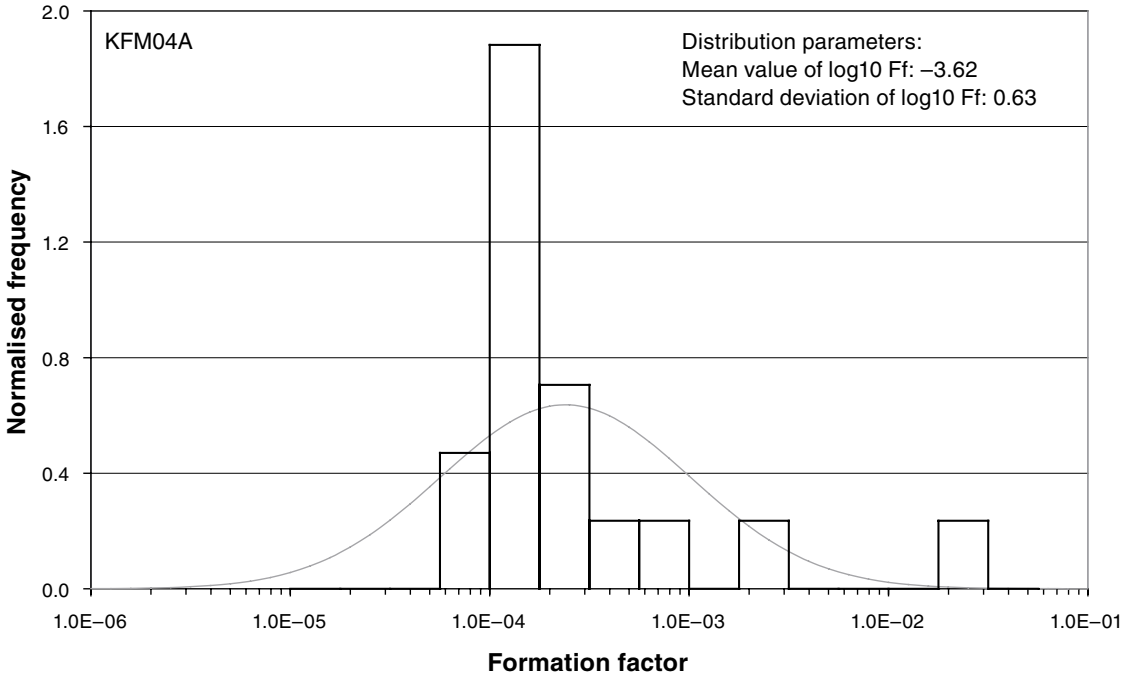

Figure 5-1. *Distribution of laboratory formation factors in KFM04A.*

5.2 In-situ rock matrix formation factor

Figure 5-2 shows the distributions of the rock matrix formation factors obtained in-situ in KFM03A and KFM04A.

The rock matrix formation factors are fairly well log-normally distributed. The rock resistivity measurements may have been somewhat affected by the limited measuring range of the in-situ tool, which would give an overestimation of the formation factors in the lower formation factor range. The mean values and standard deviations of the distributions in Figure 5-2 are provided in Table 5-1 and Table 5-2 for KFM03A and KFM04A,

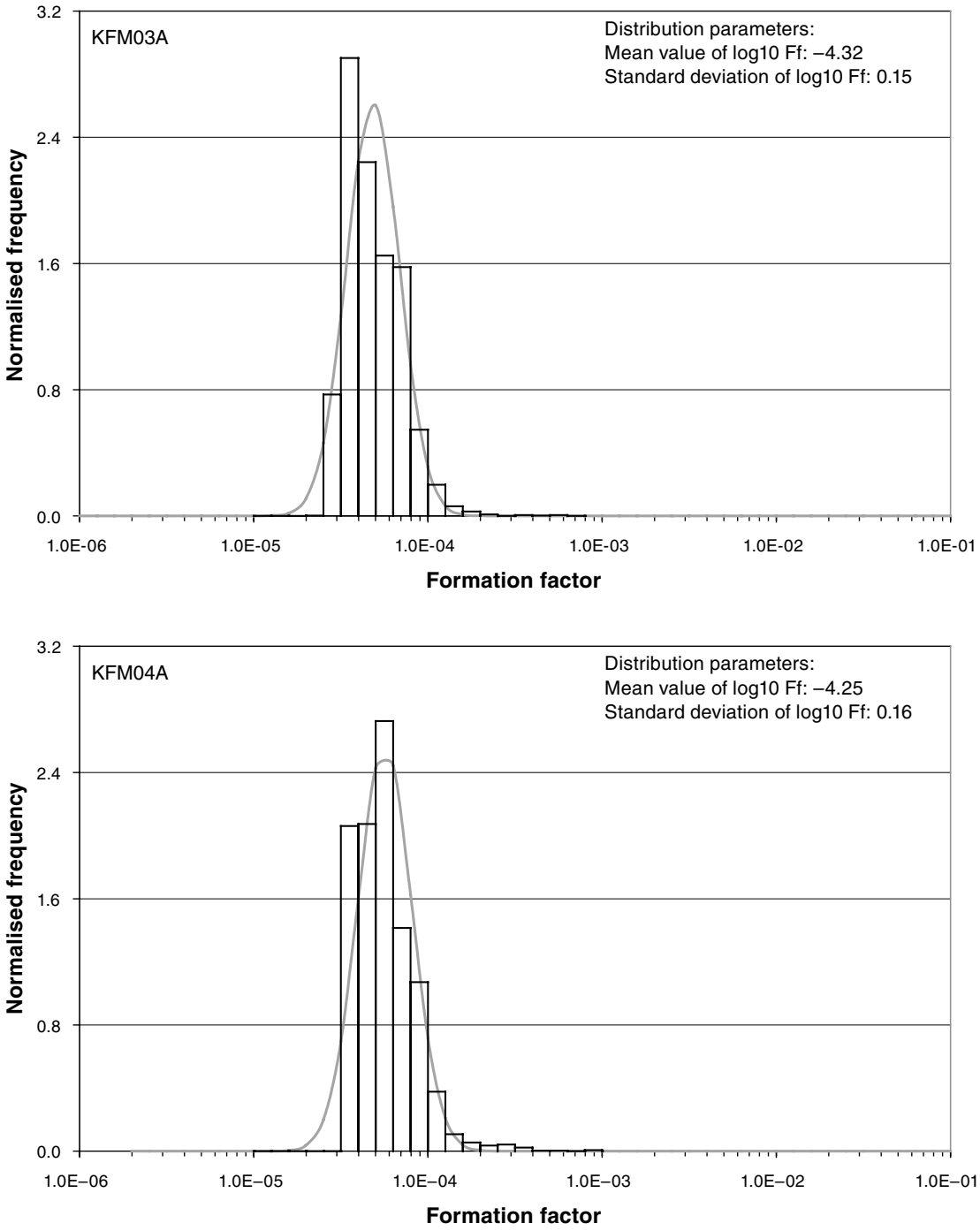

Figure 5-2. *Distributions of in-situ rock matrix formation factors in KFM03A and KFM04A.*

respectively. The in-situ rock matrix formation factor logs of KFM03A and KFM04A are displayed in Appendix C1 and C2, respectively. Rock type specific distributions of the rock matrix formation factor, for the three most abundant rock types, are shown in Appendix D1 and D3 for KFM03A and KFM04A, respectively.

5.3 In-situ fractured rock formation factor

Figure 5-3 shows the distributions of the fractured rock formation factors obtained in-situ in KFM03A and KFM04A.

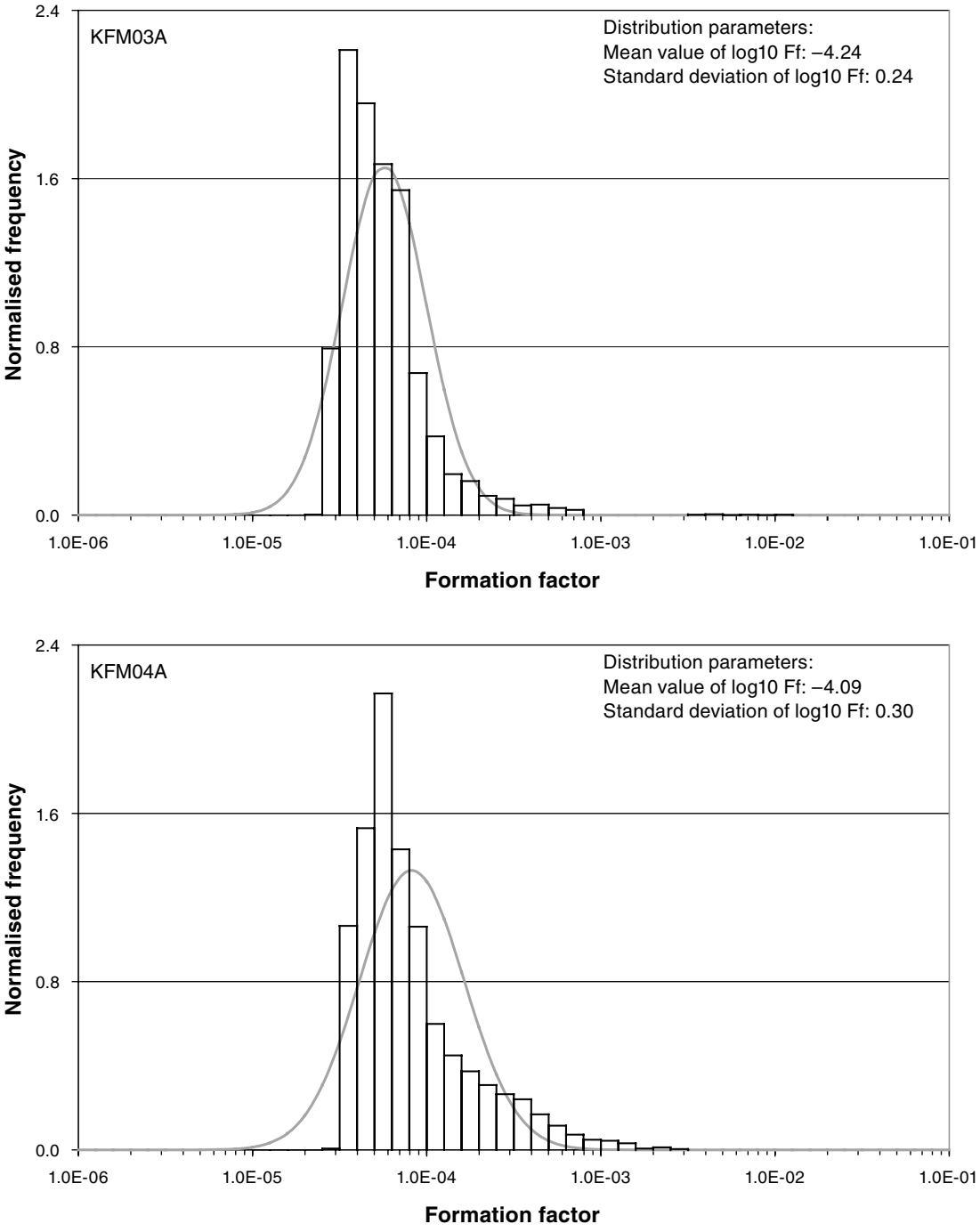

Figure 5-3. *Distributions of in-situ fractured rock formation factors in KFM03A and KFM04A.*

Except for the deviations due to the limitations in the in-situ rock resistivity tool, a deviation from the log-normal distribution can be seen in the upper formation factor region. Here, some of the obtained formation factors are affected by free water in hydraulically non-conductive fractures. The mean values and standard deviations of the distributions in Figure 5-3 are given in Table 5-1 and Table 5-2 for KFM03A and KFM04A, respectively. The in-situ fractured rock formation factor logs of KFM03A and KFM04A are shown in Appendix C1 and C2, respectively. Rock type specific distributions of the fractured rock formation factor, for the three most abundant rock types, are provided in Appendix D2 and D4 for KFM03A and KFM04A, respectively.

5.4 Comparison of formation factors of KFM03A

Table 5-1 presents mean values and standard deviations of the log-normal distributions shown in Figures 5-2 and 5-3 for KFM03A. In addition, the number of data points obtained and the arithmetic mean values for the different formation factors are presented.

As indicated in Table 5-1, the laboratory formation factors are, on average, about one order of magnitude larger than those obtained in-situ. It should be kept in mind though that the number of samples used in the laboratory is low. Therefore, not too much weight should be given to the statistical comparison.

An alternative comparison could be made if comparing each laboratory formation factor with the in-situ rock matrix formation factor, obtained at a corresponding depth. Four such comparisons are made in Appendix C3. The laboratory formation factor from a certain borehole length was compared to the mean value of the in-situ rock matrix formation factors taken within 0.5 m of that borehole length. Here, the laboratory formation factor was on average 3.6 times larger than the rock matrix formation factor.

A reason for the larger laboratory formation factor may be that the rock samples are de-stressed. The laboratory samples may also have been mechanically damaged in the drilling process and during sample preparation. In both these cases, results obtained in the laboratory may be non-conservative.

It should also be noted from Table 5-1 that the fractured rock formation factors are, on average, 1.6 times as large as the rock matrix formation factors.

Table 5-1. Distribution parameters and arithmetic mean value of the formation factor, KFM03A.

Formation factor	Number of data points	Mean $\log_{10}(F_f)$	Standard deviation $\log_{10}(F_f)$	Arithmetic mean F_f
Laboratory F_f	5			3.59×10^{-4}
In-situ Rock matrix F_f	3,951	–4.32	0.153	5.20×10^{-5}
In-situ Fractured rock F_f	7,610	–4.24	0.240	8.24×10^{-5}

5.5 Comparison of formation factors of KFM04A

Table 5-2 presents mean values and standard deviations of the log-normal distributions shown in Figures 5-1, 5-2, and 5-3 for KFM04A. In addition, the number of data points obtained and the arithmetic mean values for the different formation factors are shown.

As indicated in Table 5-2, the laboratory formation factors are, on average, more than one order of magnitude larger than the rock matrix formation factors obtained in-situ.

An alternative comparison could be made if comparing each laboratory formation factor with the in-situ rock matrix formation factor, obtained at a corresponding depth. Three such comparisons are made in Appendix C4. As for borehole KFM03A the laboratory formation factor from a certain borehole length was compared to the mean value of the in-situ rock matrix formation factors taken within 0.5 m of that borehole length. Here, the laboratory formation factor was on average 1.5 times larger than the rock matrix formation factor, cf Section 5.4.

It should also be noted from Table 5-2 that the fractured rock formation factors are, on average, 2.0 times as large as the rock matrix formation factors.

Table 5-2. Distribution parameters and arithmetic mean value of the formation factor, KFM04A.

Formation factor	Number of data points	Mean $\log_{10}(F_f)$	Standard deviation $\log_{10}(F_f)$	Arithmetic mean F_f
Laboratory F_f	17	–3.62	0.626	1.91×10^{-3}
In-situ Rock matrix F_f	3,081	–4.25	0.155	6.18×10^{-5}
In-situ Fractured rock F_f	8,263	–4.09	0.300	1.22×10^{-4}

6 Summary and discussions

The formation factors obtained in KFM03A and KFM04A range from 2.5×10^{-5} to 2.7×10^{-2}, and appear to be fairly well distributed according to the log-normal distribution. The obtained in-situ distributions, including the rock type specific distributions, have mean values for $\log_{10}(F_f)$ between –4.40 and –3.96 and standard deviations between 0.11 and 0.39. The arithmetic mean values range between 4.12×10^{-5} and 1.82×10^{-4}. In general, similar distributions were obtained for different boreholes and different rock types.

The fractured rock formation factors were on average about twice as large as the rock matrix formation factors. This indicates that the retention capacity for non-sorbing species due to open, but hydraulically non-conductive, fractures may be as large as that of the intact rock matrix.

Judging from the obtained formation factor histograms, a fairly large fraction of the obtained in-situ rock resistivities may have been affected by limitations of the in-situ rock resistivity tool. However, these limitations have only minor effects on the obtained arithmetic mean values of the formation factor.

The formation factors obtained in the laboratory are, on average, about one order of magnitude larger than those obtained in-situ. However, in the seven comparisons made between laboratory formation factors and in-situ rock matrix formation factors at corresponding depths, that laboratory formation factor is, on average, only 2.7 times larger.

This indicates either that the porous system is compressed in-situ or that the laboratory samples become mechanically damaged when brought to the laboratory. In both these cases the laboratory results would be non-conservative.

References

/1/ **Nielsen U T, Ringgaard J, 2004.** Geophysical borehole logging in borehole KFM02A, KFM03A and KFM03B. SKB P-04-97, Svensk Kärnbränslehantering AB.

/2/ **Nielsen U T, Ringgaard J, 2004.** Geophysical borehole logging in borehole KFM04A, KFM06A, HFM10, HFM11, HFM12 and HFM13. SKB P-04-144, Svensk Kärnbränslehantering AB.

/3/ **Pöllänen J, Sokolnicki M, 2004.** Difference flow logging in borehole KFM03A. SKB P-04-189, Svensk Kärnbränslehantering AB.

/4/ **Rouhiainen P, Pöllänen J, 2004.** Difference flow logging in borehole KFM04A. SKB P-04-190, Svensk Kärnbränslehantering AB.

/5/ **Löfgren M, Neretnieks I, in prep.** Formation factor logging in-situ and in the laboratory by electrical methods in KSH01A and KSH02: Measurements and evaluation of methodology. SKB P-05-27, Svensk Kärnbränslehantering AB.

/6/ **Wacker P, Bergelin A, Berg C, 2004.** Hydrochemical characterisation in KFM03A: Results from six investigated sections: 386.0–391.0, 448.0–453.0 m, 448.5–455.6 m, 639.0–646.1 m, 939.5–946.6 m, 980.0–1,001.2 m. SKB P-04-108, Svensk Kärnbränslehantering AB.

/7/ **Wacker P, Bergelin A, Berg C, 2004.** Hydrochemical characterisation in KFM04A: Results from two investigated borehole sections, 230.5–237.6 and 354.0–361.1 metres. SKB P-04-109, Svensk Kärnbränslehantering AB.

/8/ **Petersson J, Wängnerud A, Danielsson P, 2003**. Boremap mapping of telescopic drilled borehole KFM03A and core drilled borehole KFM03B. SKB P-03-116, Svensk Kärnbränslehantering AB.

/9/ **Petersson J, Wängnerud A, Berglund J, Danielsson P, 2004**. Boremap mapping of telescopic drilled borehole KFM04A. SKB P-04-115, Svensk Kärnbränslehantering AB.

/10/ **Ehrenborg J, Stejskal V, 2004**. Boremap mapping of core drilled boreholes KSH01A and KSH01B. SKB P-04-01, Svensk Kärnbränslehantering AB.

/11/ **Löfgren M, Neretnieks I, in prep.** Formation factor logging in-situ and in the laboratory by electrical methods in KFM01A and KFM02A: Measurements and evaluation of methodology. Site investigation report P-05-29, Svensk Kärnbränslehantering AB.

/12/ **Löfgren M, Neretnieks I, 2002.** Formation factor logging in-situ by electrical methods. Background and methodology. SKB TR-02-27, Svensk Kärnbränslehantering AB.

/13/ **Löfgren M, 2001.** Formation factor logging in igneous rock by electrical methods. Licentiate thesis at the Royal Institute of Technology, Stockholm, Sweden. ISBN 91-7283-207-x.

/14/ **Ohlsson Y, 2000.** Studies of Ionic Diffusion in Crystalline Rock. Doctoral thesis at the Royal Institute of Technology, Stockholm, Sweden. ISBN 91-7283-025-5.

/15/ **Löfgren M, 2004.** Diffusive properties of granitic rock as measured by in-situ electrical methods. Doctoral thesis at the Royal Institute of Technology, Stockholm, Sweden. ISBN 91-7283-935-X.

/16/ **Wacker P, Bergelin A, Nilsson A-C, 2003.** Complete hydrochemical characterisation in KFM01A: Results from two investigated sections, 110.1–120.8 and 176.8–183.9 metres. SKB P-03-94, Svensk Kärnbränslehantering AB.

/17/ **Rouhiainen P, Pöllänen J, 2004.** Difference flow logging in borehole KFM02A. SKB P-04-188, Svensk Kärnbränslehantering AB.

/18/ **Wacker P, Bergelin A, Nilsson A-C, 2004.** Hydrochemical characterisation in KFM02A: Results from three investigated borehole sections, 106.5–126.5, 413.5–433.5 and 509.0–516.1 m. SKB P-04-70, Svensk Kärnbränslehantering AB.

/19/ **Pöllänen J, Sokolnicki M, Rouhiainen P, 2004.** Difference flow logging in borehole KFM05A. SKB P-04-191, Svensk Kärnbränslehantering AB.

/20/ **Laaksoharju M, Gimeno M, Auqué L, Gómez J, Smellie J, Tullborg E-L, Gurban I, 2004.** Hydrogeochemical evaluation of the Forsmark site, model version 1.1. SKB R-04-05, Svensk Kärnbränslehantering AB.

/21/ **Johnson RA, 1994.** Miller and Freund's probability & statistics for engineers, 5ed. Prentice-Hall Inc., ISBN 0-13-721408-1.

Appendix A

Appendix A1: Laboratory formation factor for rock samples from KFM03A

Secup (m)	Formation factor
76.74	3.19E–04
311.45	4.06E–05
367.44	4.39E–04
660.41	9.01E–04
957.67	9.72E–05

Secup = upper position in borehole for sample.

Appendix A2: Laboratory formation factor for rock samples from KFM04A

Secup (m)	Formation factor
120.02	7.17E–04
140.02	1.10E–04
180.05	1.80E–04
199.95	6.58E–05
220.02	1.75E–04
239.70	2.69E–02
260.07	2.02E–04
300.02	9.33E–05
319.12	1.13E–04
339.86	1.64E–04
359.29	1.26E–04
379.95	9.34E–05
400.02	1.56E–04
420.27	2.79E–03
459.95	4.02E–04
479.96	7.11E–05
499.96	1.28E–04

Secup = upper position in borehole.

Appendix B1: In-situ rock resistivities and fractures KFM03A

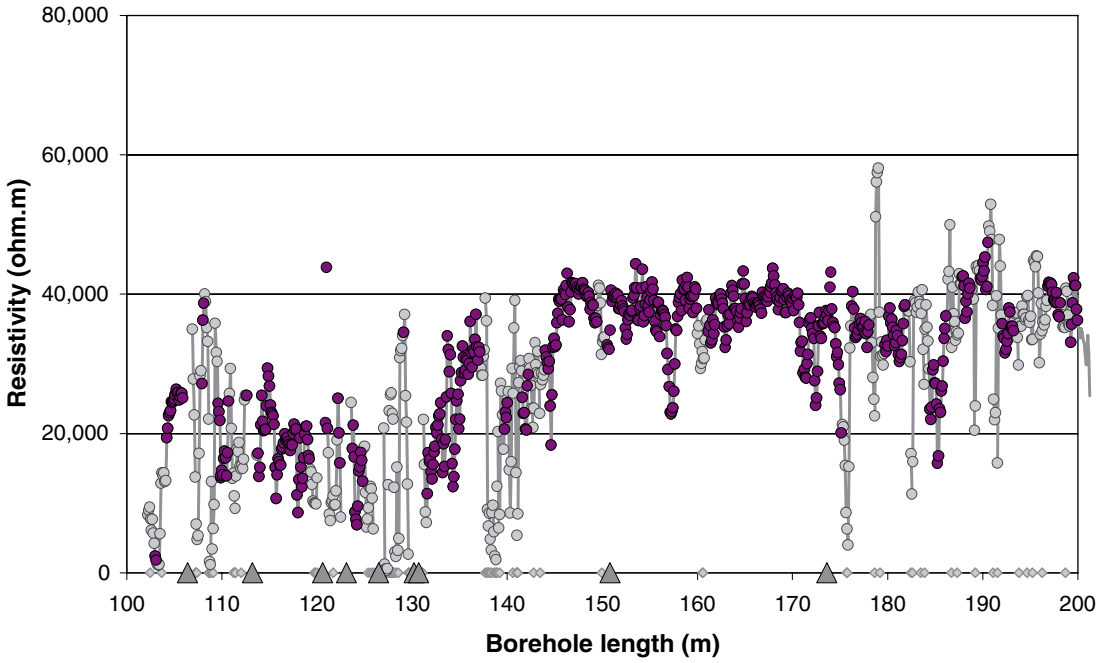

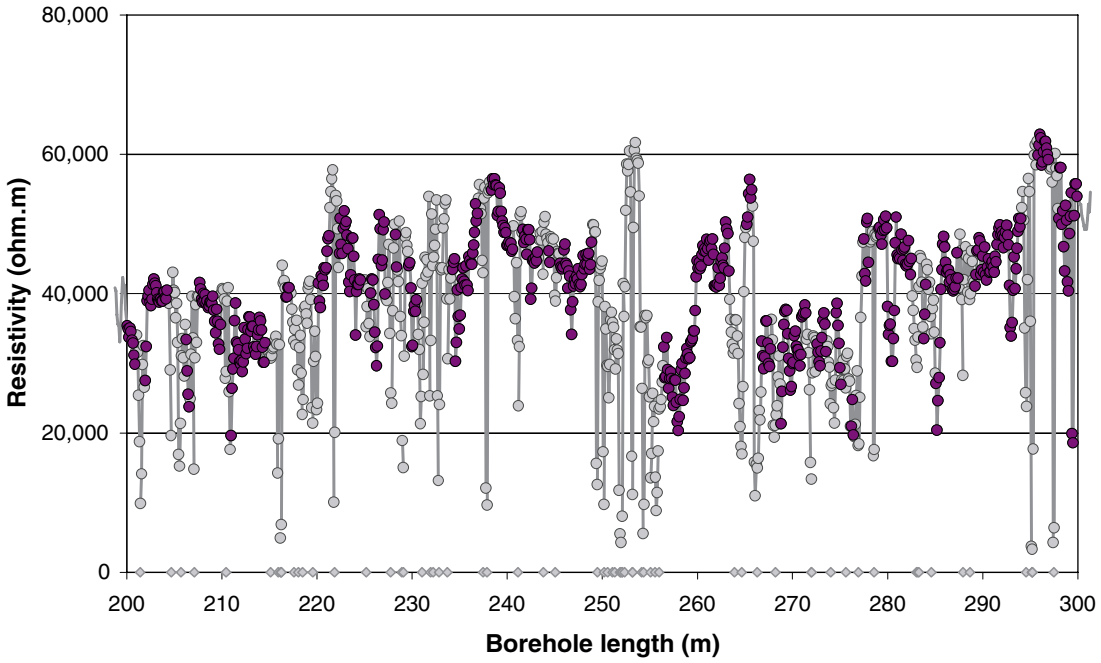

Fractured rock resistivity
Rock matrix resistivity
Location of broken fracture parting the drill core
Location of hydraulically conductive fracture detected in the difference flow logging

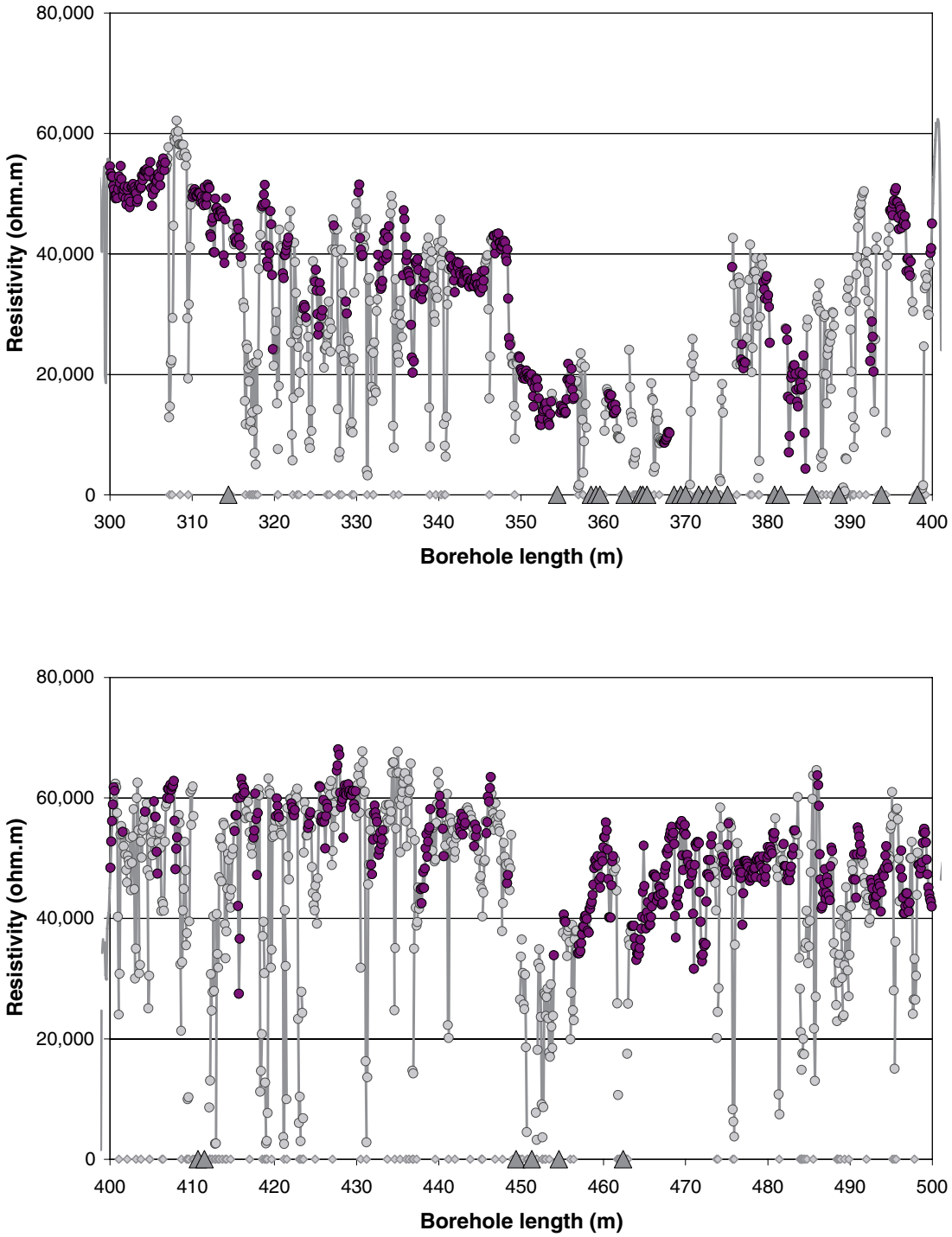
80,000
60,000
40,000
20,000
0
Resistivity (ohm.m)
300
310
320
330
340
350
360
370
380
390
400
Borehole length (m)
80,000
60,000
40,000
20,000
0
Resistivity (ohm.m)
400
410
420
430
440
450
460
470
480
490
500
Borehole length (m)
Fractured rock resistivity
Rock matrix resistivity
Location of broken fracture parting the drill core
Location of hydraulically conductive fracture detected in the difference flow logging

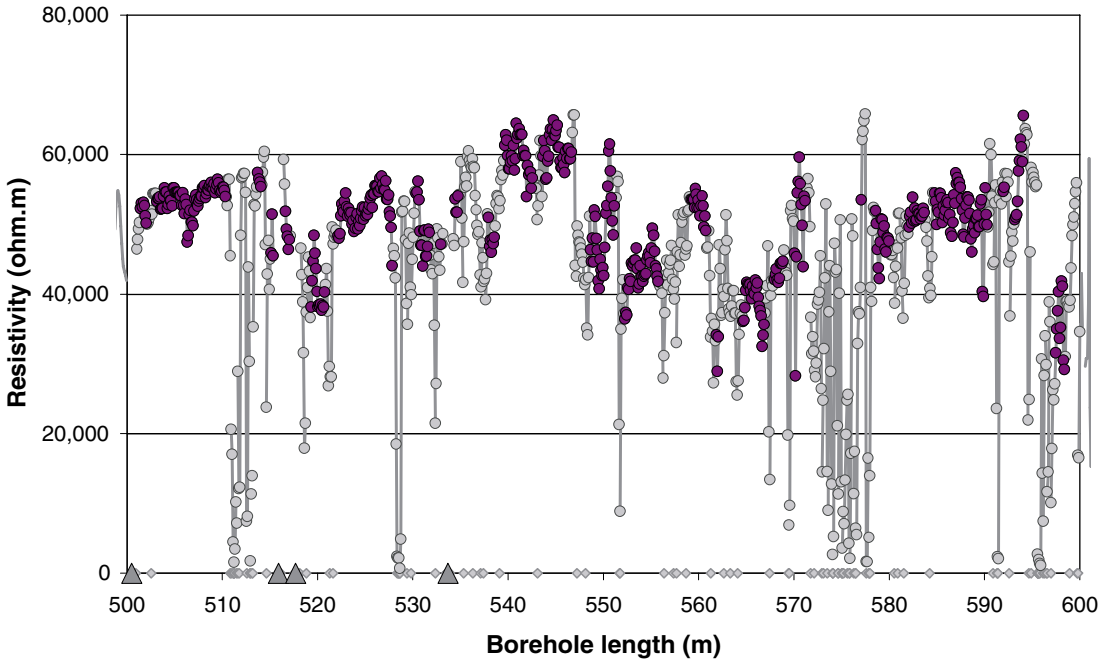

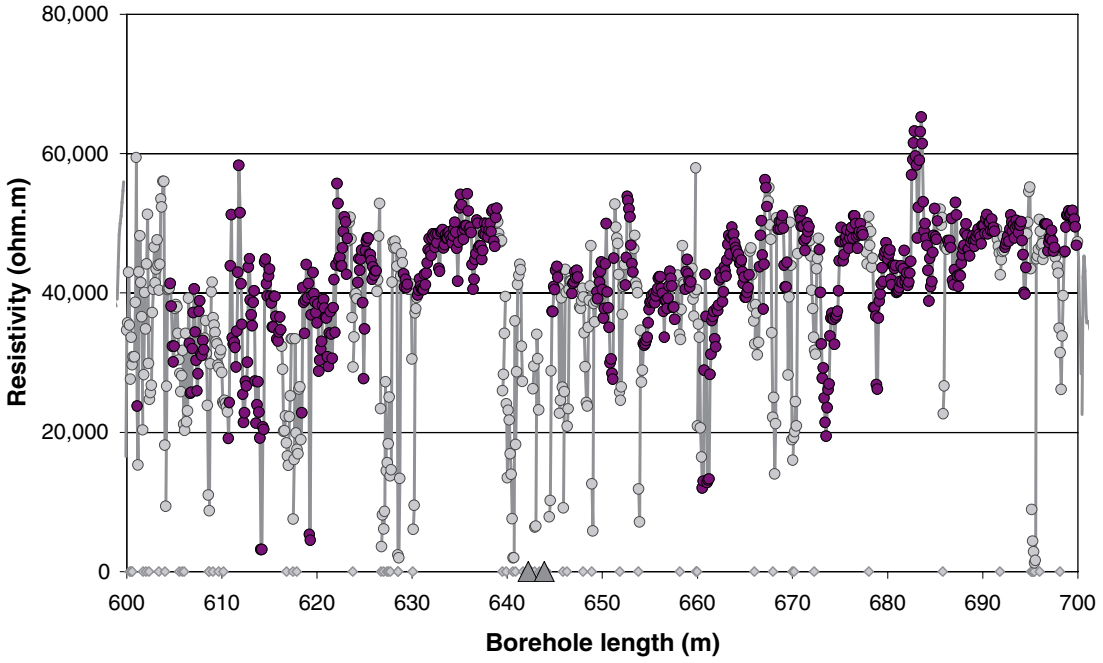

Fractured rock resistivity
Rock matrix resistivity
Location of broken fracture parting the drill core
Location of hydraulically conductive fracture detected in the difference flow logging

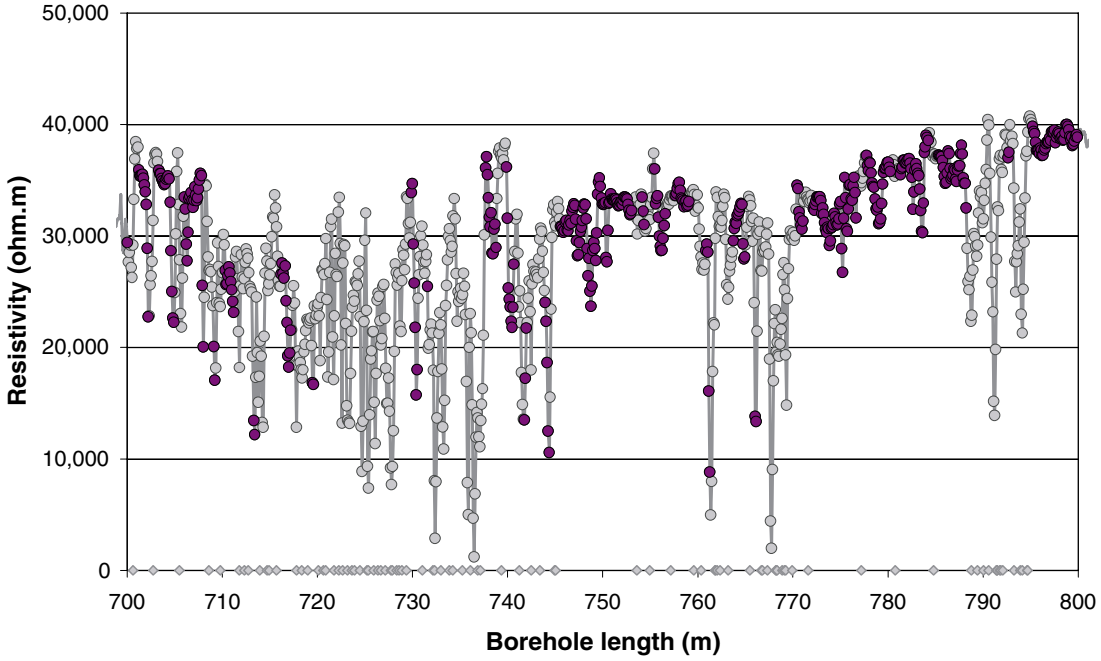

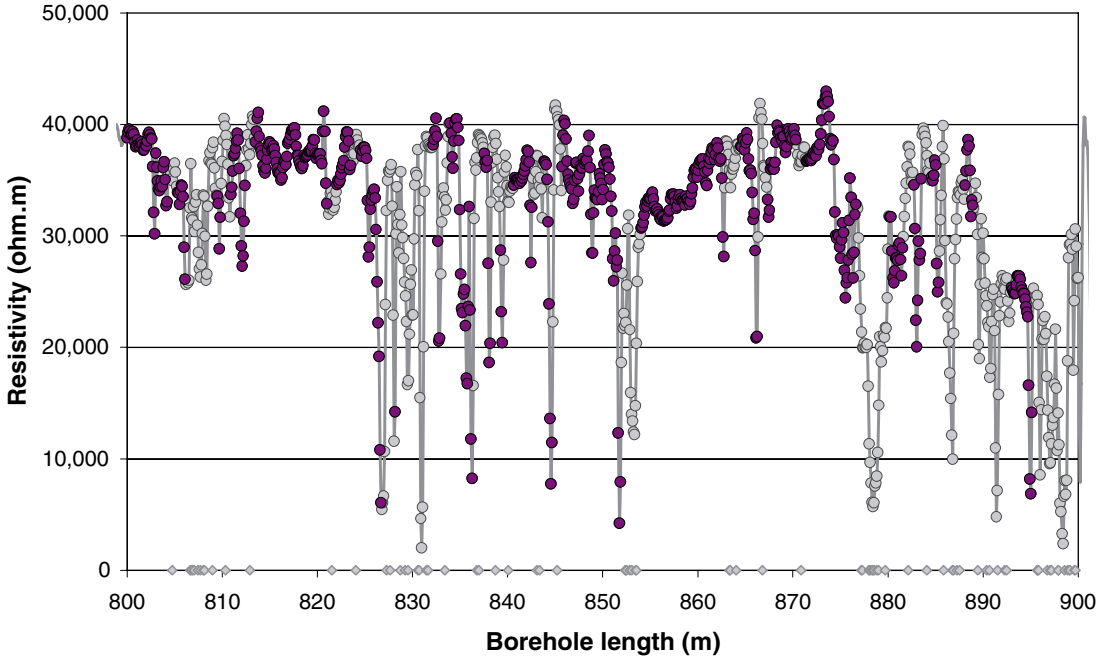

Fractured rock resistivity
Rock matrix resistivity
Location of broken fracture parting the drill core
Location of hydraulically conductive fracture detected in the difference flow logging

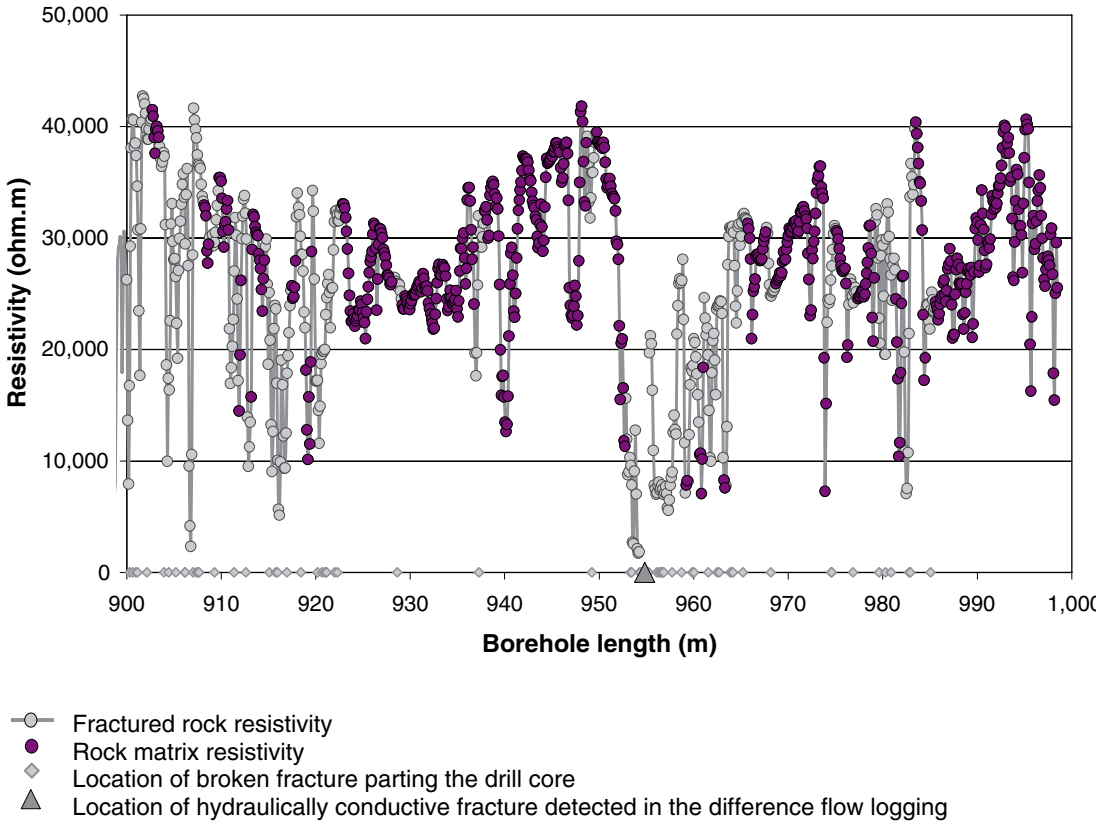

Fractured rock resistivity
Rock matrix resistivity
Location of broken fracture parting the drill core
Location of hydraulically conductive fracture detected in the difference flow logging

Appendix B2: In-situ rock resistivities and fractures KFM04A

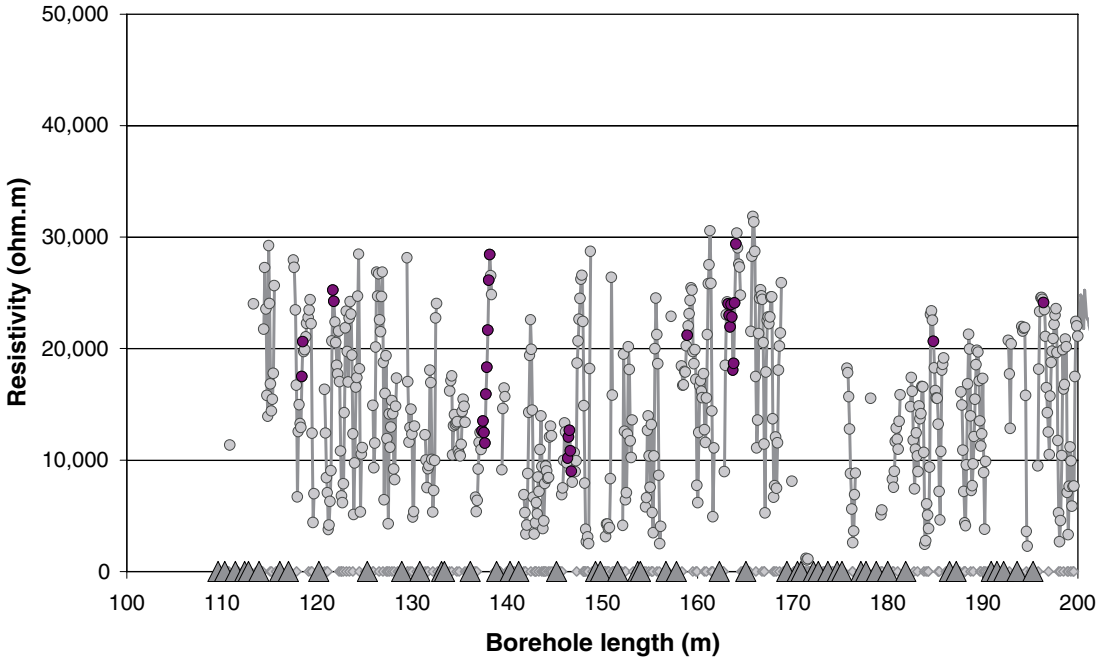

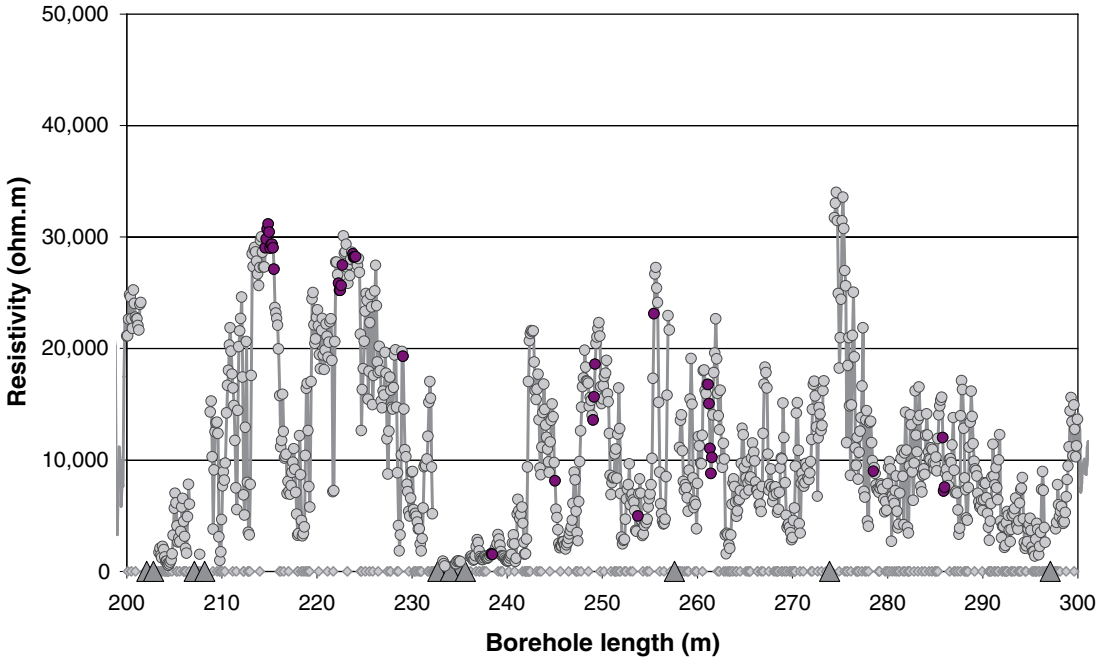

Fractured rock resistivity
Rock matrix resistivity
Location of broken fracture parting the drill core
Location of hydraulically conductive fracture detected in the difference flow logging

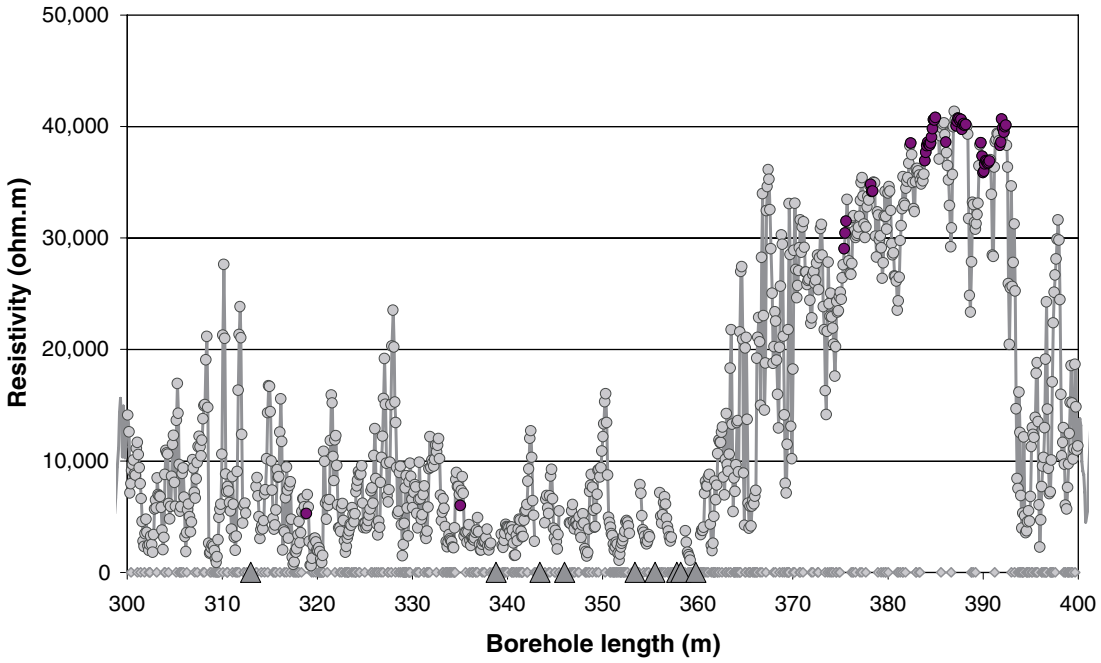

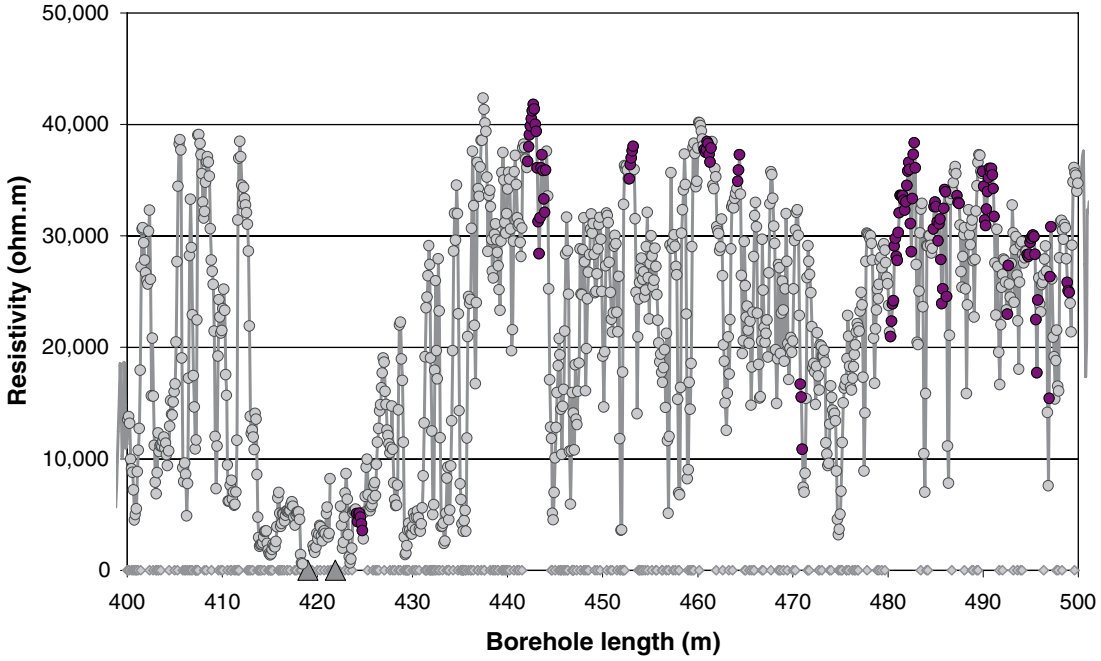

Fractured rock resistivity
Rock matrix resistivity
Location of broken fracture parting the drill core
Location of hydraulically conductive fracture detected in the difference flow logging

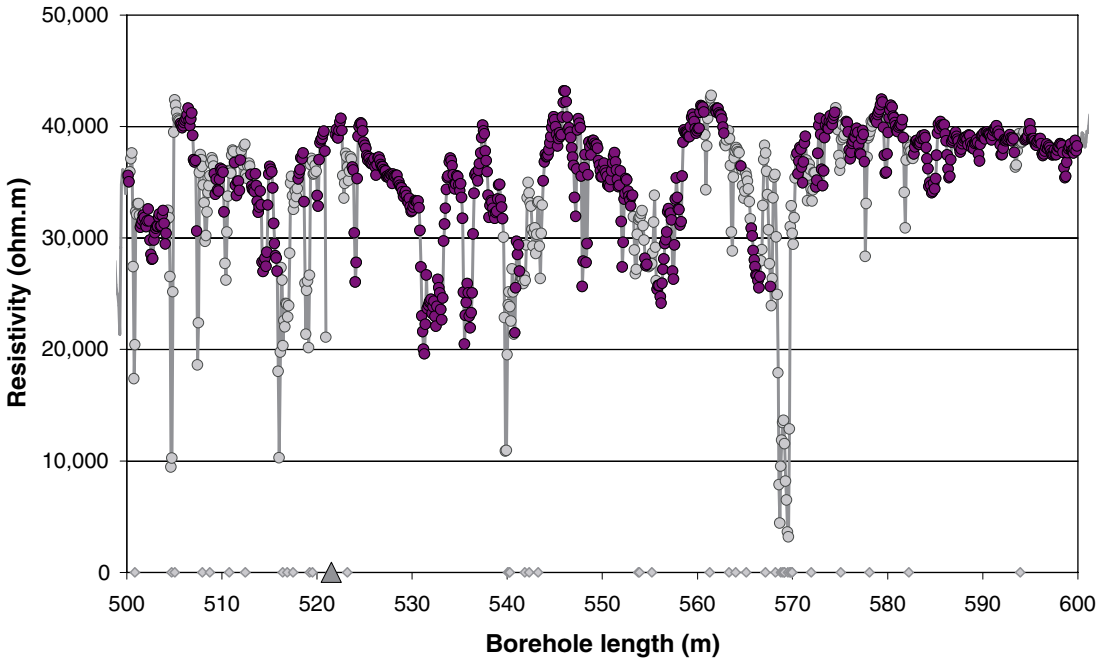

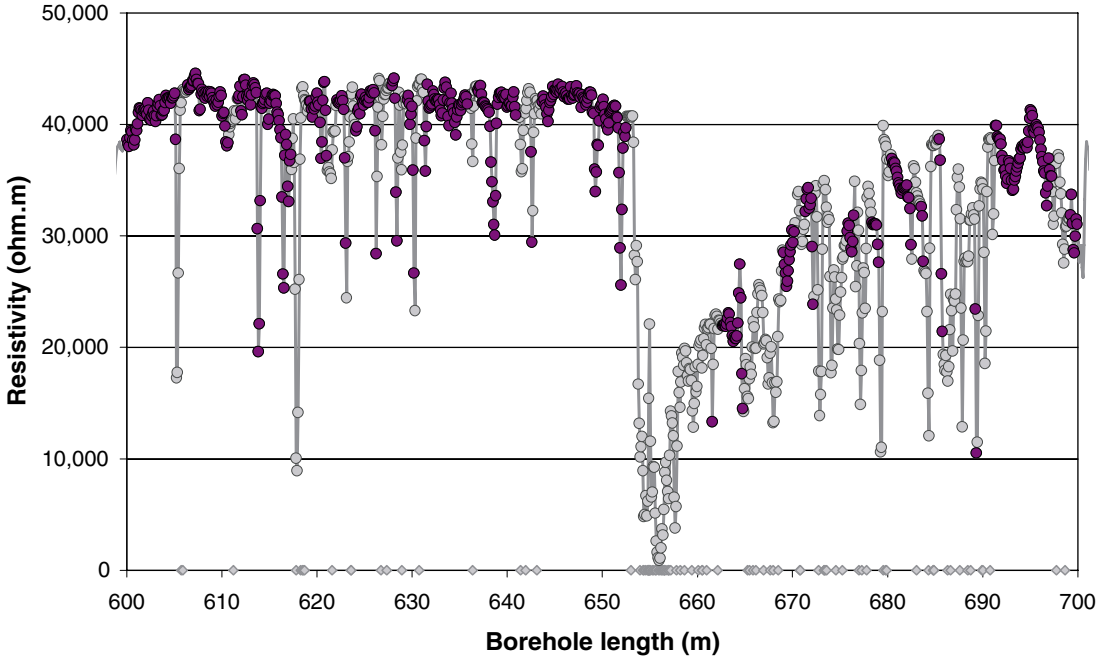

Fractured rock resistivity
Rock matrix resistivity
Location of broken fracture parting the drill core
Location of hydraulically conductive fracture detected in the difference flow logging

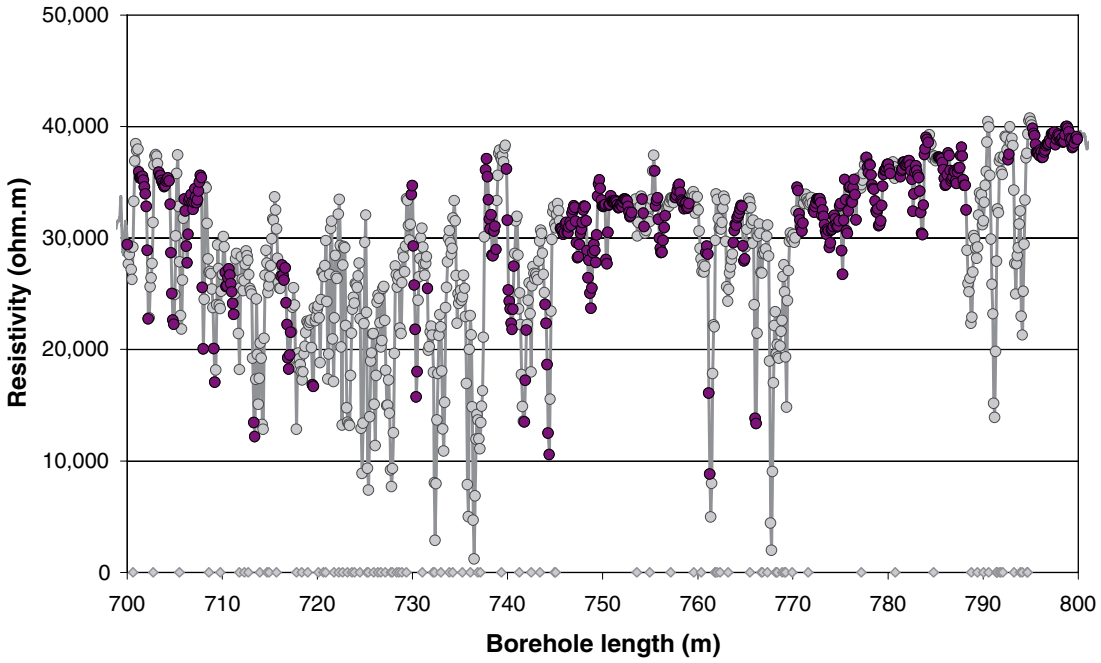

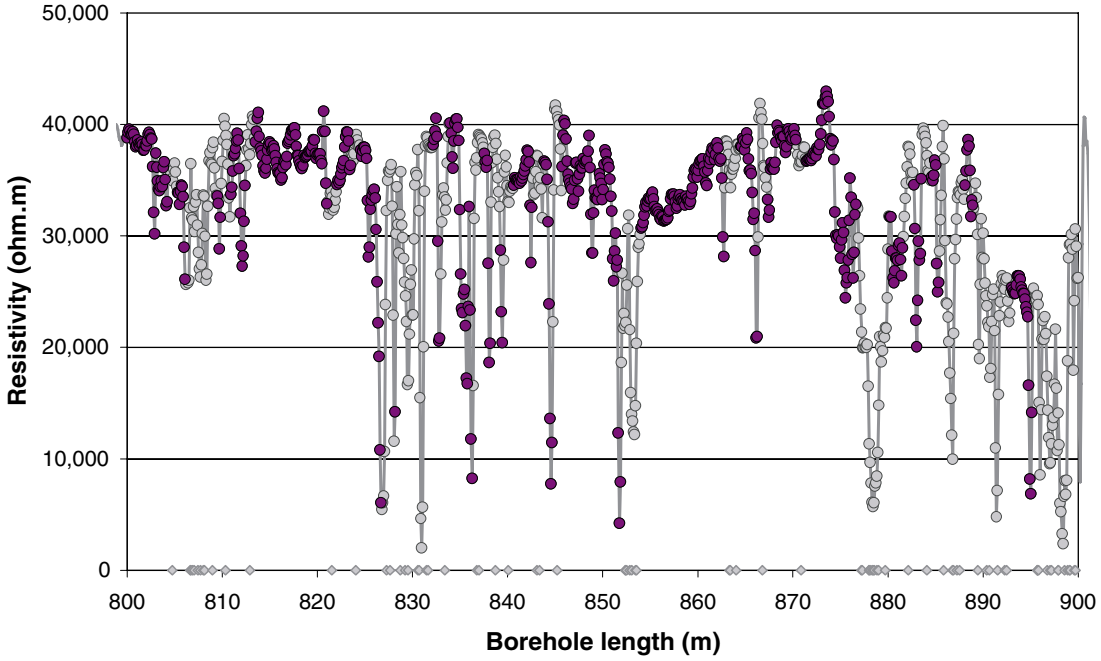

Fractured rock resistivity
Rock matrix resistivity
Location of broken fracture parting the drill core
Location of hydraulically conductive fracture detected in the difference flow logging

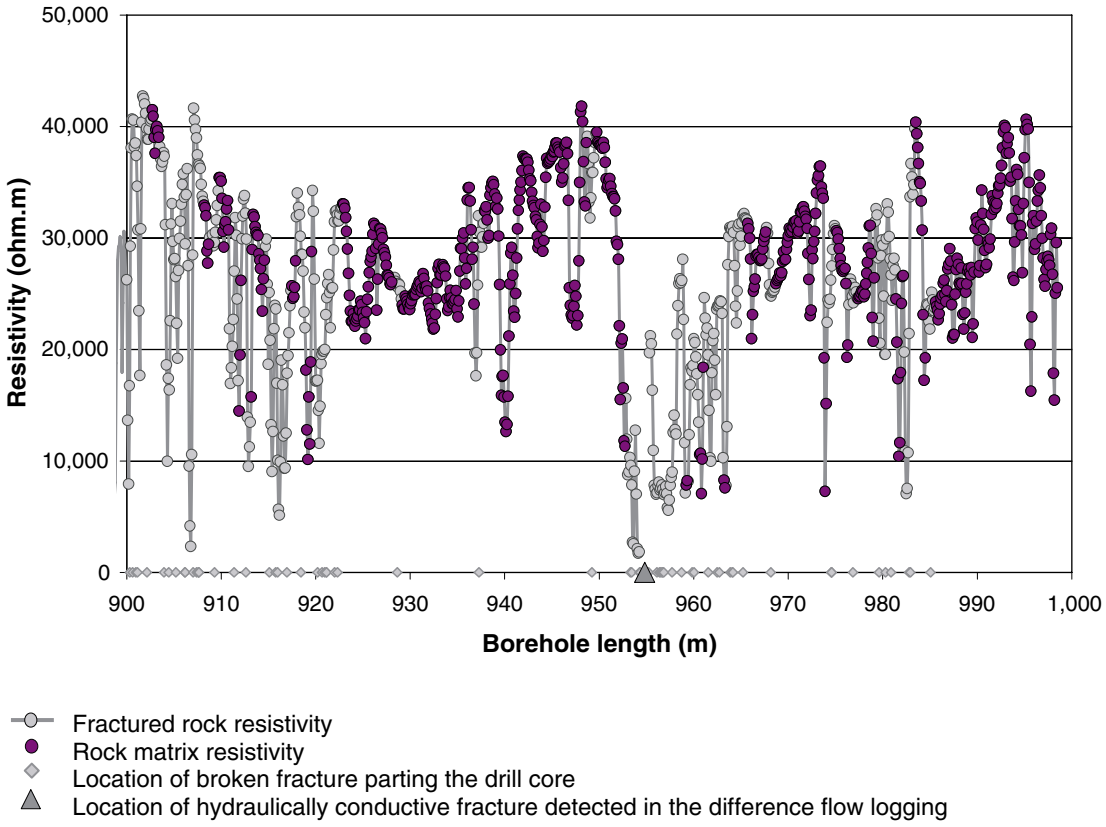
50,000
40,000
30,000
20,000
10,000
0
Resistivity (ohm.m)
900
910
920
930
940
950
960
970
980
990
1,000
Borehole length (m)
Fractured rock resistivity
Rock matrix resistivity
Location of broken fracture parting the drill core
Location of hydraulically conductive fracture detected in the difference flow logging

Appendix C

Appendix C1: In-situ and laboratory formation factors KFM03A

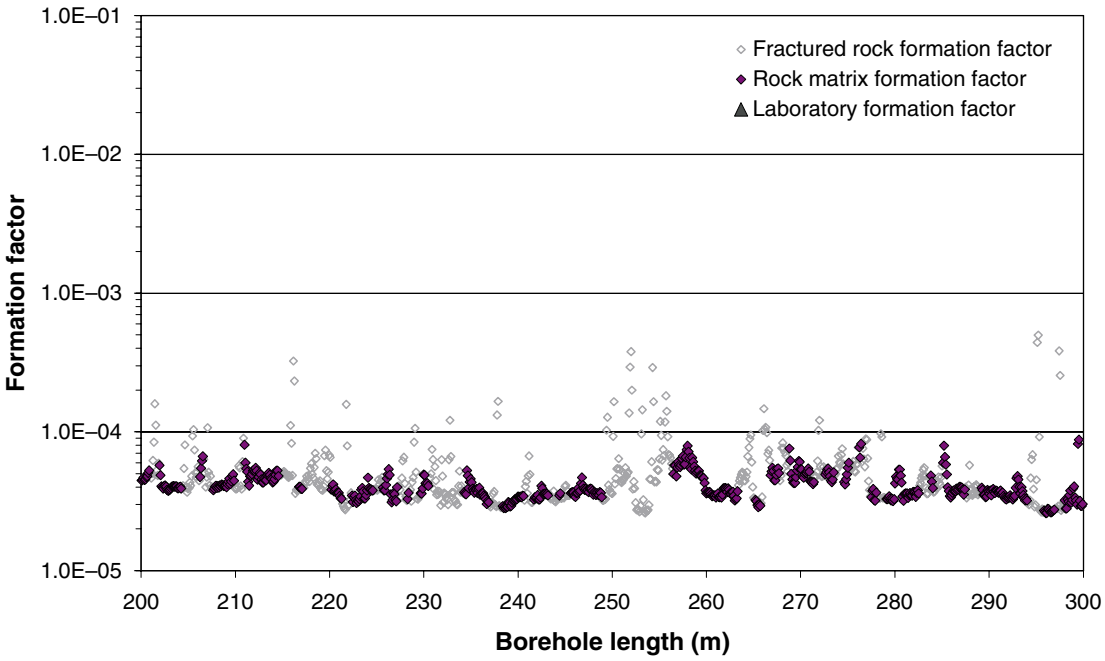

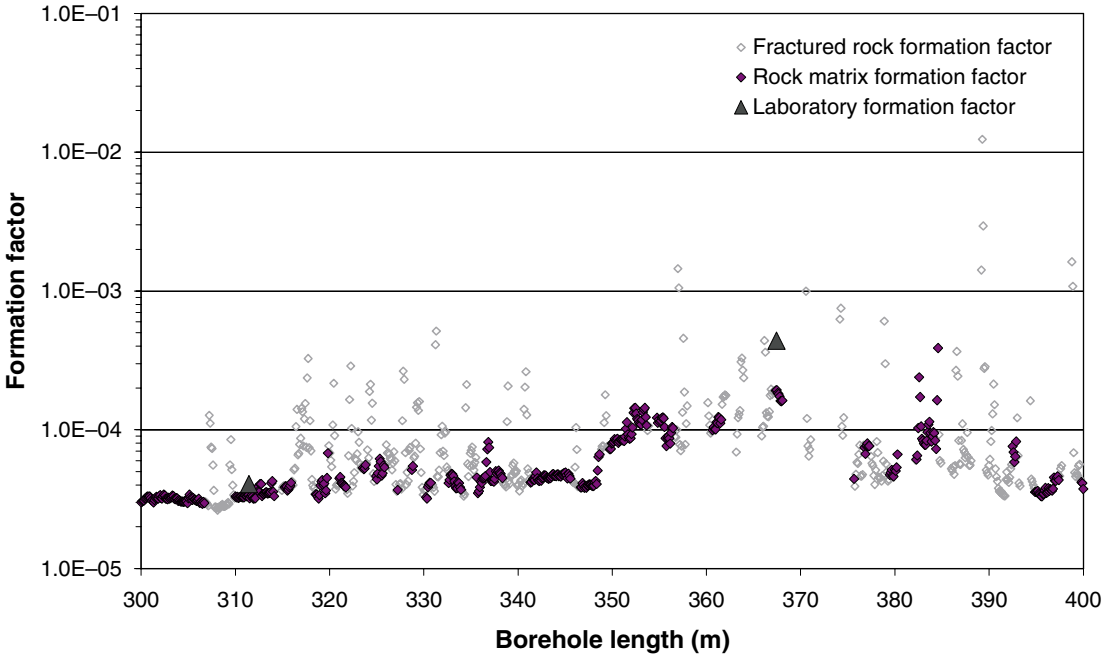

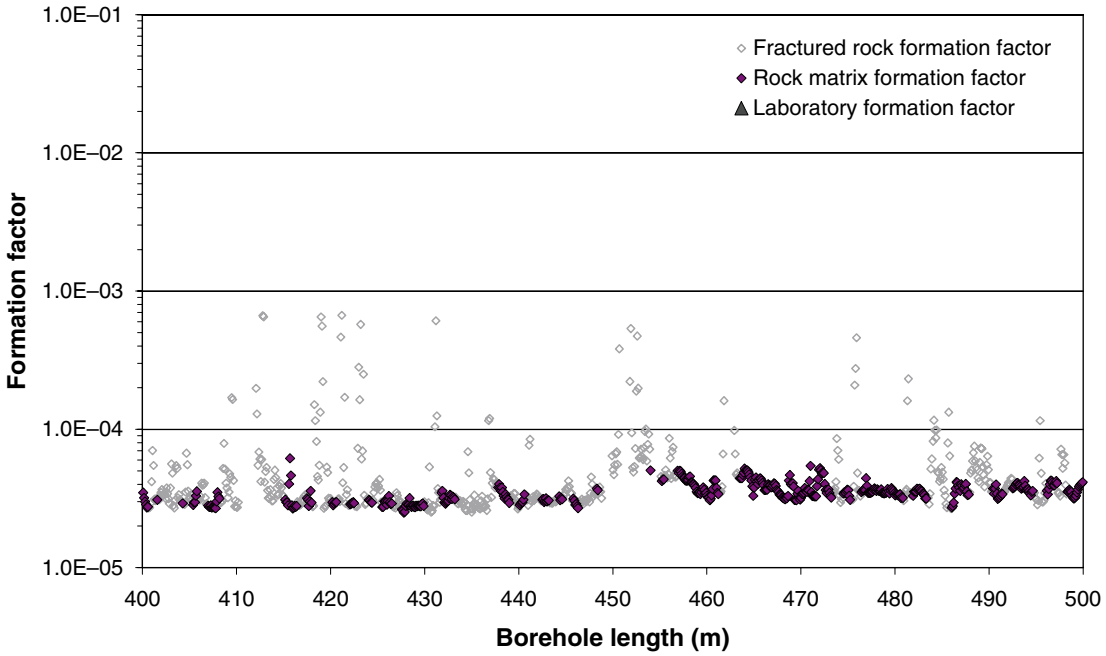
Fractured rock formation factor
Rock matrix formation factor
Laboratory formation factor
Formation factor
1.0E–01
1.0E–02
1.0E–03
1.0E–04
1.0E–05
400
410
420
430
440
450
460
470
480
490
500
Borehole length (m)

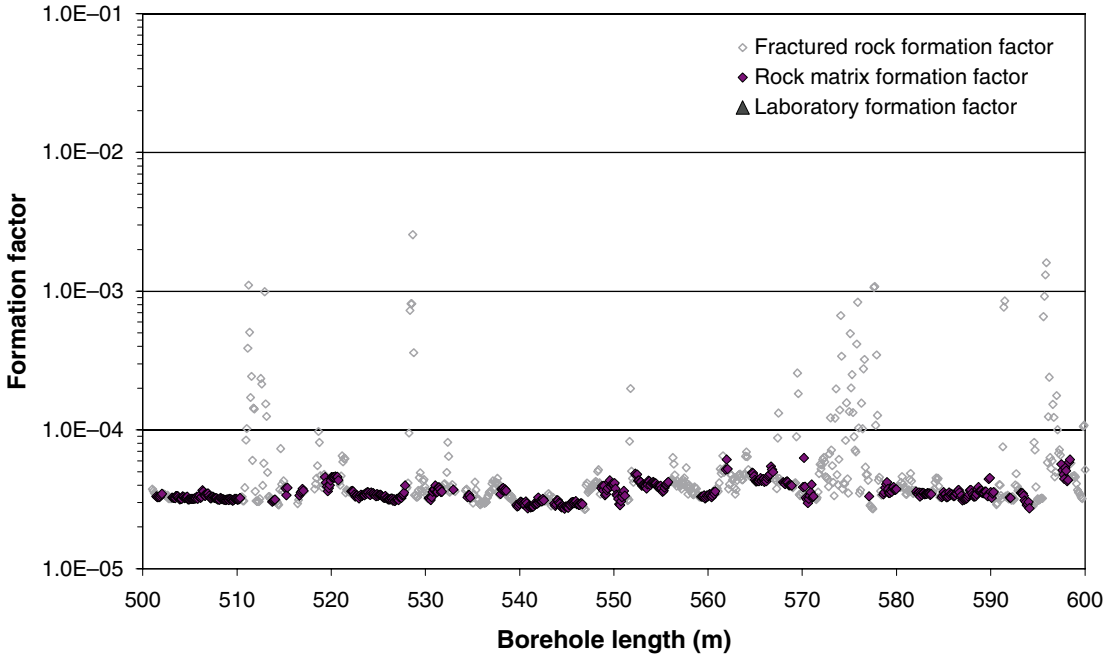
Fractured rock formation factor
Rock matrix formation factor
Laboratory formation factor
Formation factor
1.0E–01
1.0E–02
1.0E–03
1.0E–04
1.0E–05
500
510
520
530
540
550
560
570
580
590
600
Borehole length (m)

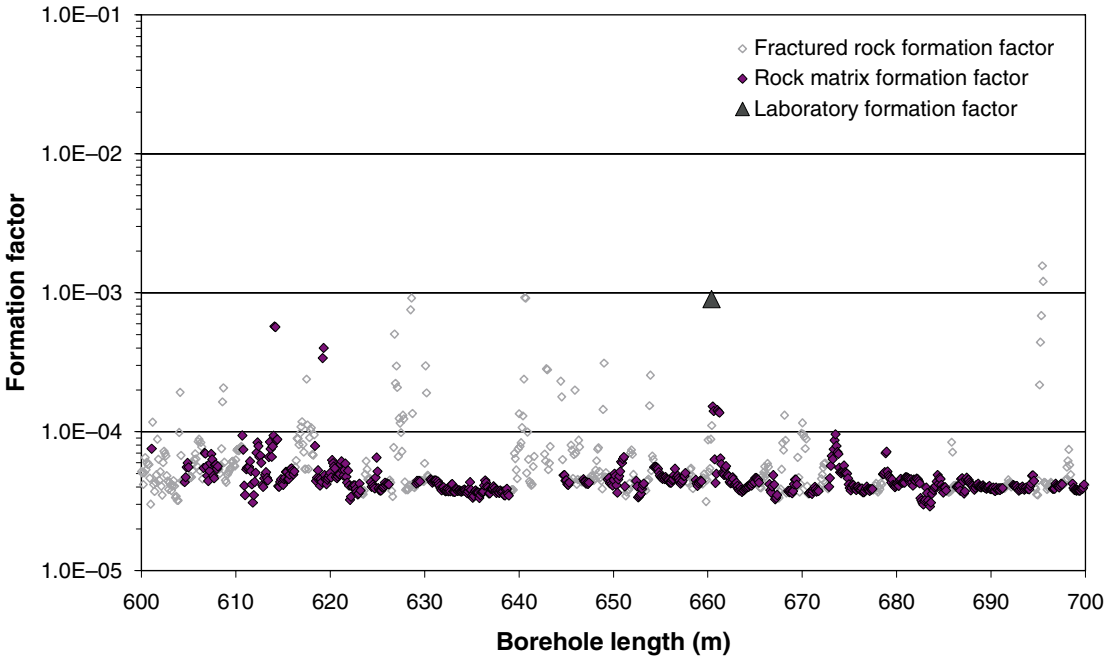
1.0E–01
1.0E–02
1.0E–03
1.0E–04
1.0E–05
Formation factor
Fractured rock formation factor
Rock matrix formation factor
Laboratory formation factor
600
610
620
630
640
650
660
670
680
690
700
Borehole length (m)

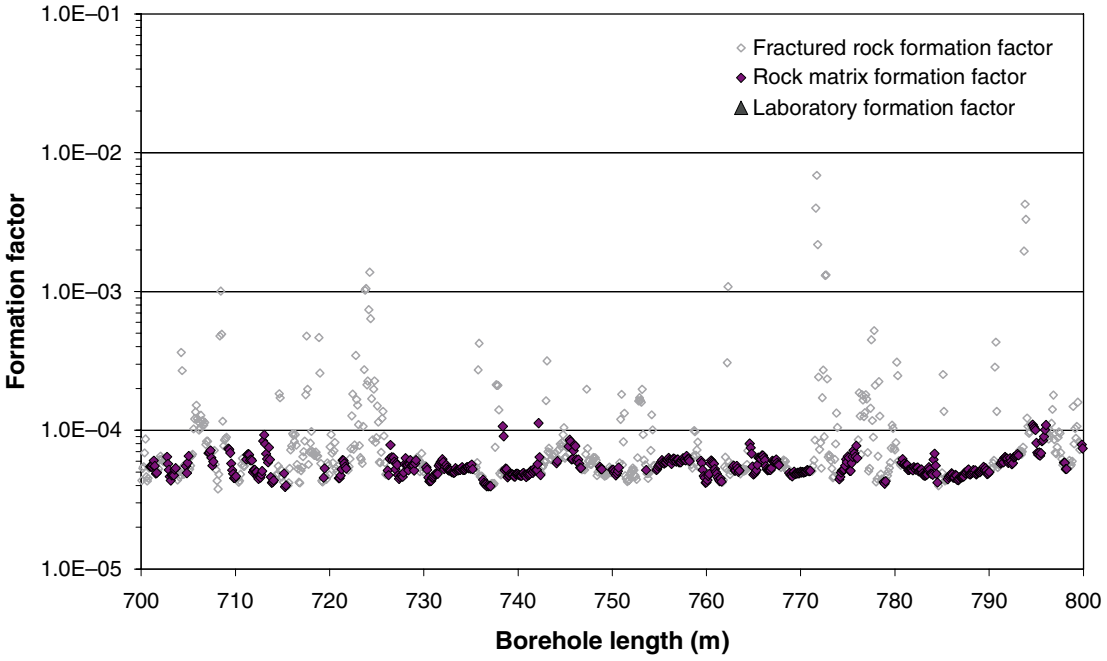
1.0E–01
1.0E–02
1.0E–03
1.0E–04
1.0E–05
Formation factor
Fractured rock formation factor
Rock matrix formation factor
Laboratory formation factor
700
710
720
730
740
750
760
770
780
790
800
Borehole length (m)

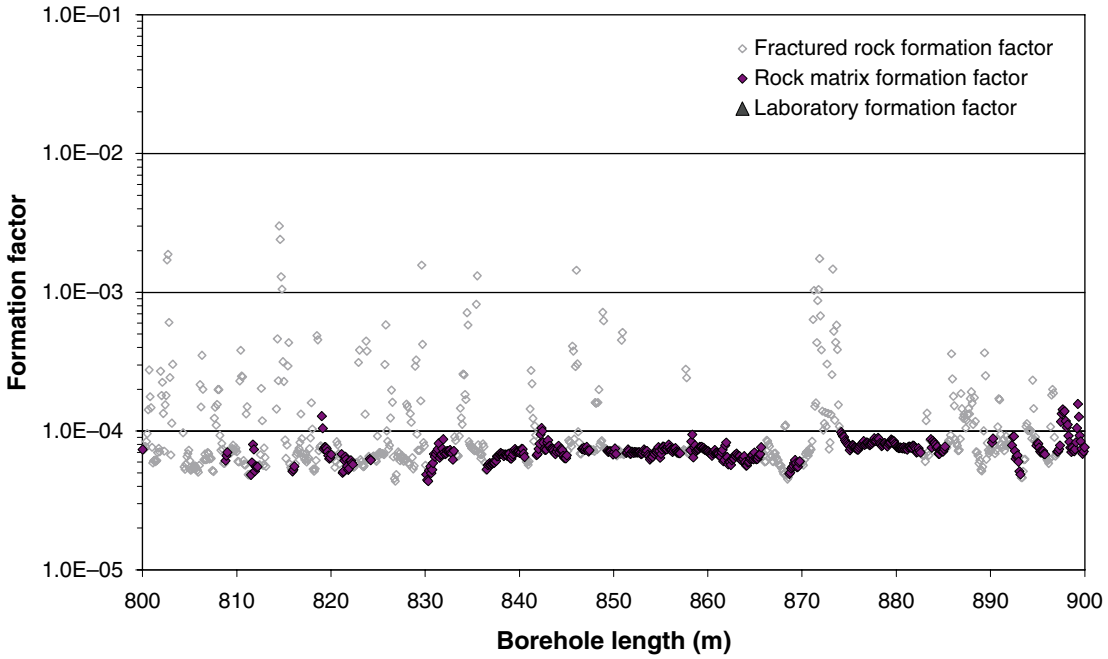
1.0E–01
1.0E–02
1.0E–03
1.0E–04
1.0E–05
Formation factor
Fractured rock formation factor
Rock matrix formation factor
Laboratory formation factor
800
810
820
830
840
850
860
870
880
890
900
Borehole length (m)

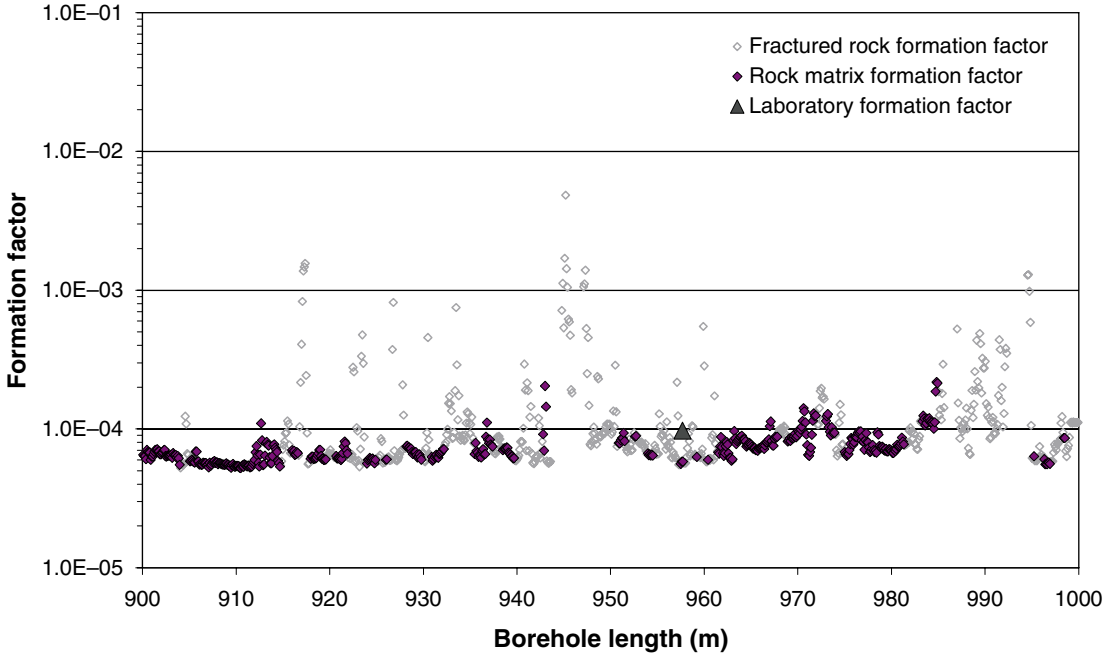
1.0E–01
1.0E–02
1.0E–03
1.0E–04
1.0E–05
Formation factor
Fractured rock formation factor
Rock matrix formation factor
Laboratory formation factor
900
910
920
930
940
950
960
970
980
990
1000
Borehole length (m)

Appendix C2: In-situ and laboratory formation factors KFM04A

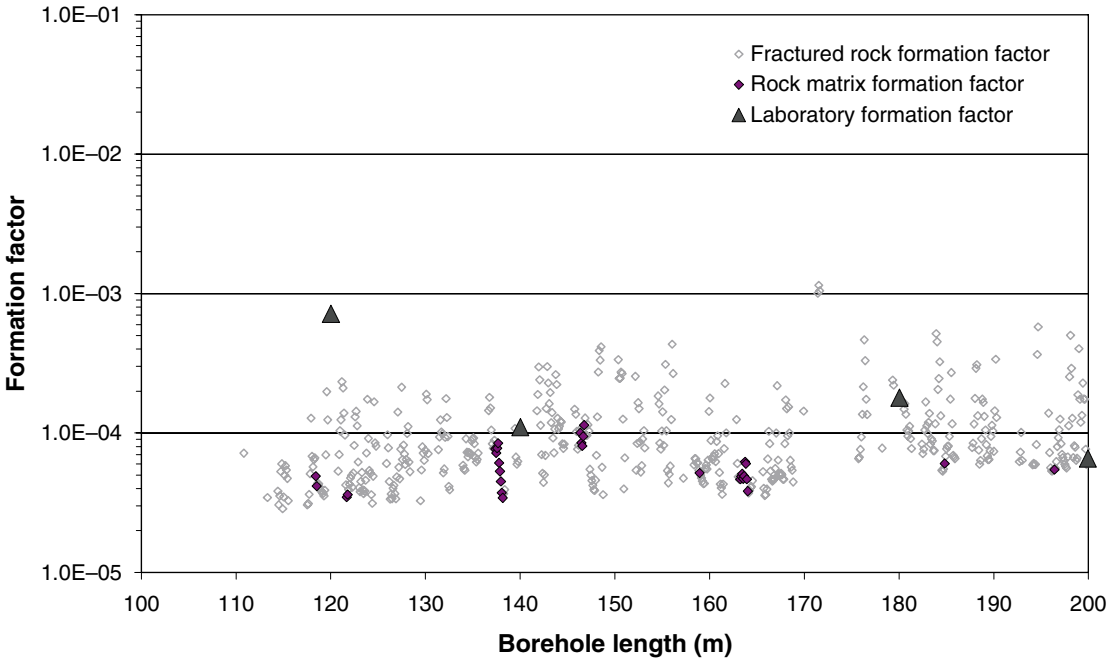

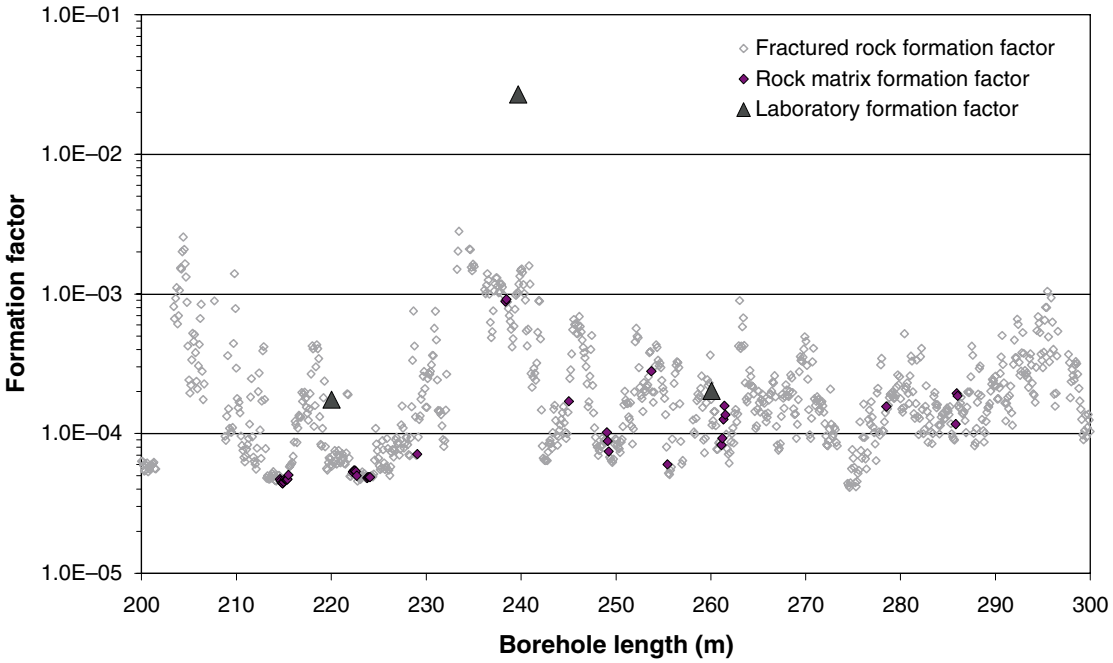

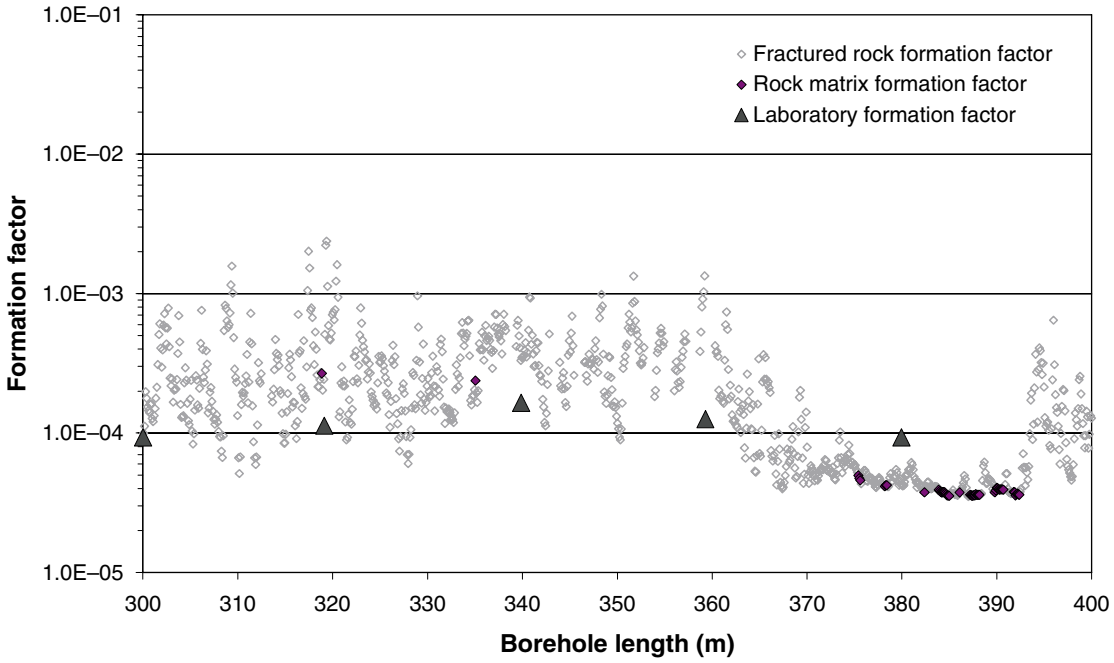
1.0E–01
1.0E–02
1.0E–03
1.0E–04
1.0E–05
Formation factor
300
310
320
330
340
350
360
370
380
390
400
Borehole length (m)
Fractured rock formation factor
Rock matrix formation factor
Laboratory formation factor

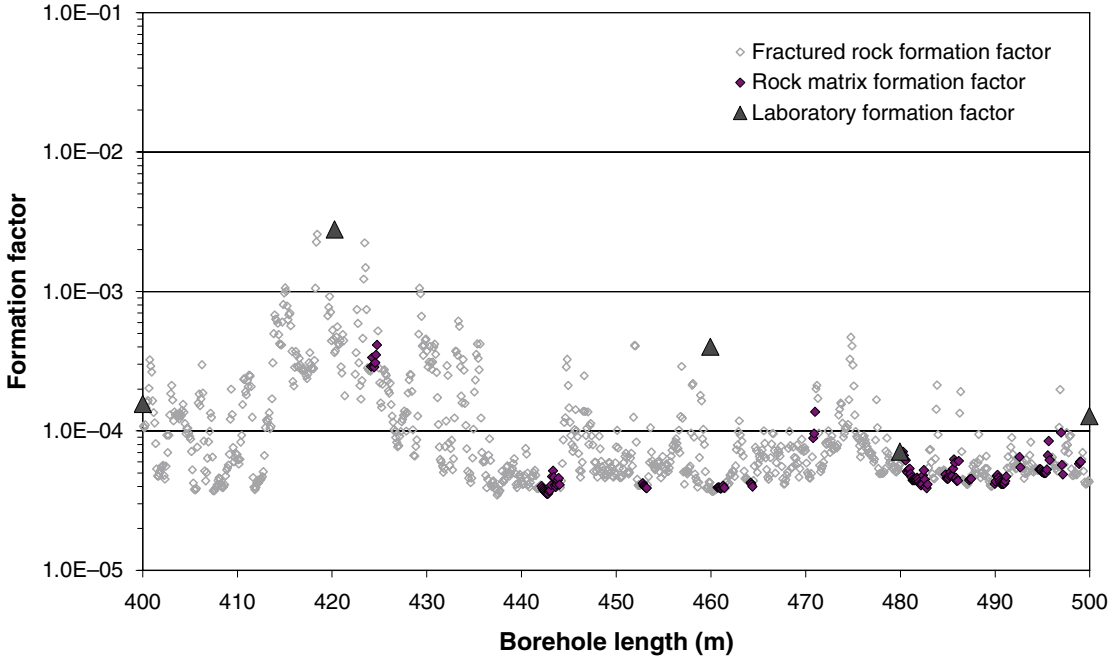
1.0E–01
1.0E–02
1.0E–03
1.0E–04
1.0E–05
Formation factor
400
410
420
430
440
450
460
470
480
490
500
Borehole length (m)
Fractured rock formation factor
Rock matrix formation factor
Laboratory formation factor

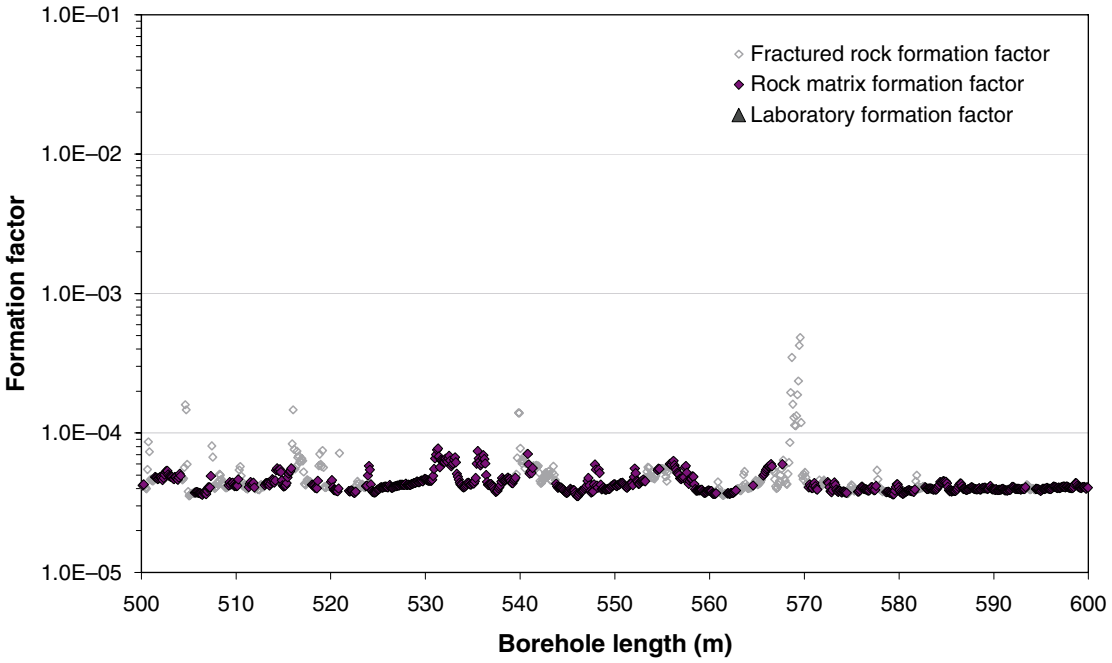
Fractured rock formation factor
Rock matrix formation factor
Laboratory formation factor
Formation factor
1.0E–01
1.0E–02
1.0E–03
1.0E–04
1.0E–05
500
510
520
530
540
550
560
570
580
590
600
Borehole length (m)

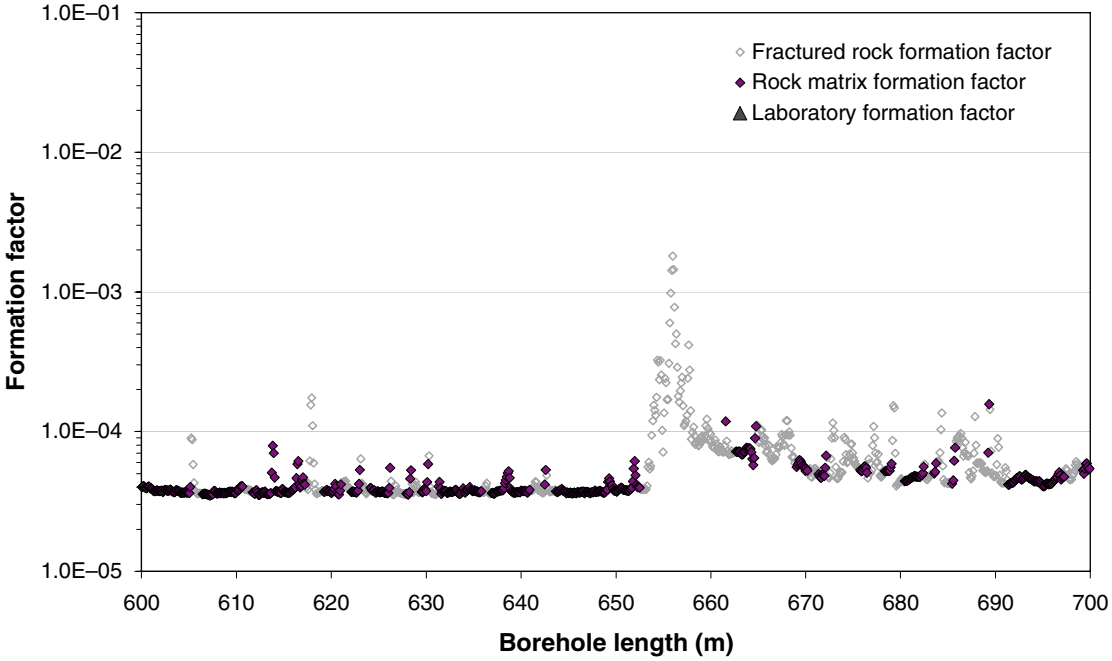
Fractured rock formation factor
Rock matrix formation factor
Laboratory formation factor
Formation factor
1.0E–01
1.0E–02
1.0E–03
1.0E–04
1.0E–05
600
610
620
630
640
650
660
670
680
690
700
Borehole length (m)

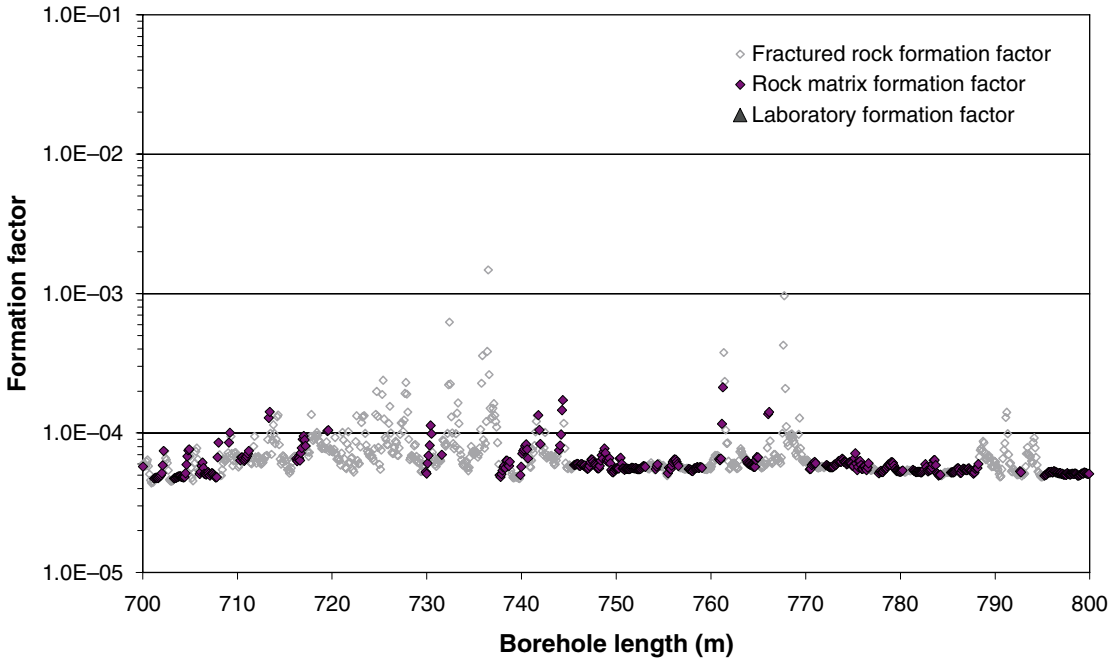
1.0E–01
1.0E–02
1.0E–03
1.0E–04
1.0E–05
Formation factor
Fractured rock formation factor
Rock matrix formation factor
Laboratory formation factor
700
710
720
730
740
750
760
770
780
790
800
Borehole length (m)

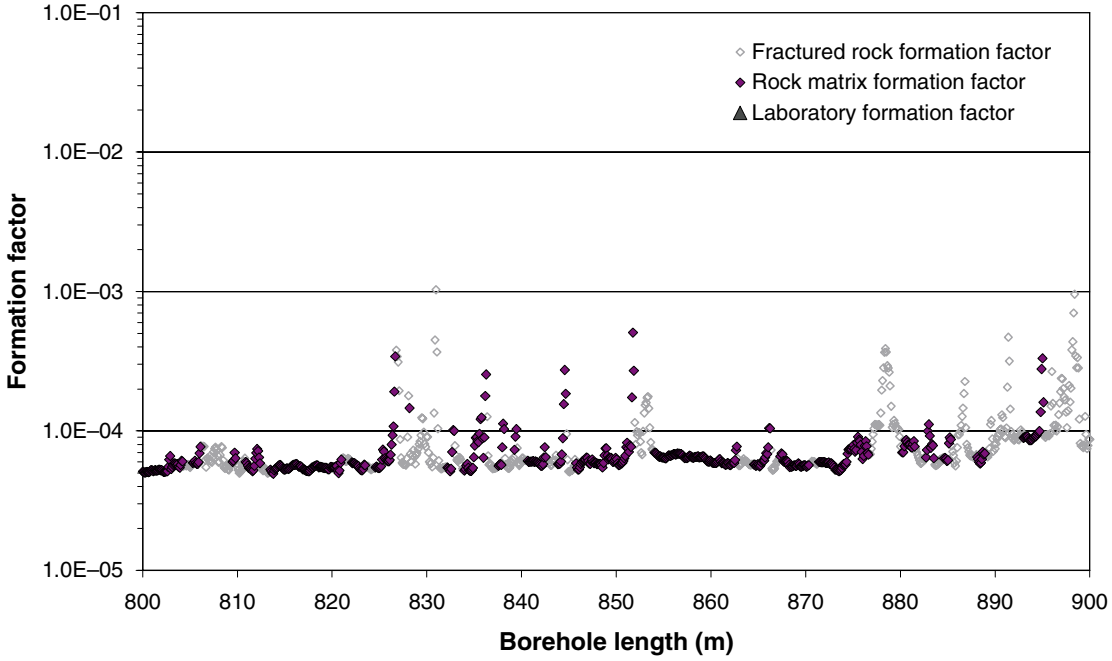
1.0E–01
1.0E–02
1.0E–03
1.0E–04
1.0E–05
Formation factor
Fractured rock formation factor
Rock matrix formation factor
Laboratory formation factor
800
810
820
830
840
850
860
870
880
890
900
Borehole length (m)

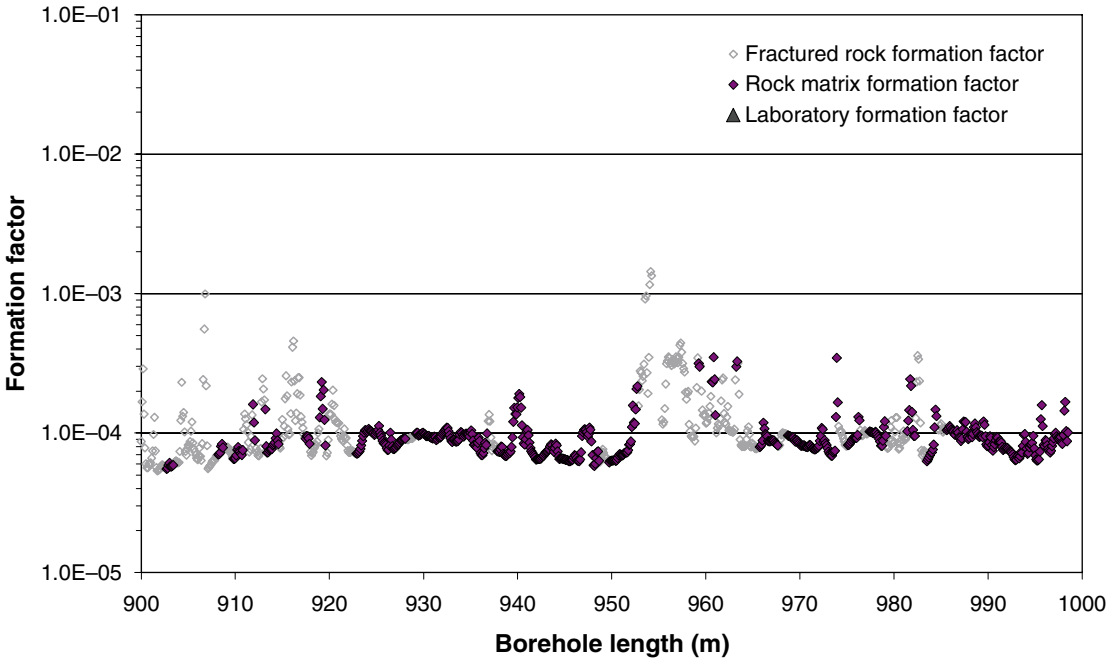
1.0E–01
1.0E–02
1.0E–03
1.0E–04
1.0E–05
Formation factor
900
910
920
930
940
950
960
970
980
990
1000
Borehole length (m)
Fractured rock formation factor
Rock matrix formation factor
Laboratory formation factor

Appendix C3: Comparison of laboratory and in-situ formation factors KFM03A

Borehole length (m)	Laboratory F_f	Rock matrix F_f	Ratio laboratory/ Rock matrix F_f
76.74	3.19E–04	–	–
311.45	4.06E–05	3.32E–05	1.2
367.44	4.39E–04	1.81E–04	2.4
660.41	9.01E–04	9.96E–05	9.0
957.67	9.72E–05	5.74E–05	1.7

Laboratory F_f = Formation factor obtained in the laboratory.
Rock matrix F_f = Arithmetic mean value of in-situ rock matrix formation factors from within 0.5 m of the borehole length.

Appendix C4: Comparison of laboratory and in-situ formation factors KFM04A

Borehole length (m)	Laboratory F_f	Rock matrix F_f	Ratio laboratory/ Rock matrix F_f
120.02	7.17E–04	–	–
140.02	1.10E–04	–	–
180.05	1.80E–04	–	–
199.95	6.58E–05	–	–
220.02	1.75E–04	–	–
239.70	2.69E–02	–	–
260.07	2.02E–04	–	–
300.02	9.33E–05	–	–
319.12	1.13E–04	2.68E–04	0.42
339.86	1.64E–04	–	–
359.29	1.26E–04	–	–
379.95	9.34E–05	–	–
400.02	1.56E–04	–	–
420.27	2.79E–03	–	–
459.95	4.02E–04	–	–
479.96	7.11E–05	6.80E–05	1.0
499.96	1.28E–04	4.25E–05	3.0

Laboratory F_f = Formation factor obtained in the laboratory.
Rock matrix F_f = Mean value of in-situ rock matrix formation factors from within 0.5 m of the borehole length.

Appendix D

Appendix D1: Rock type specific distributions of rock matrix formation factors KFM03A

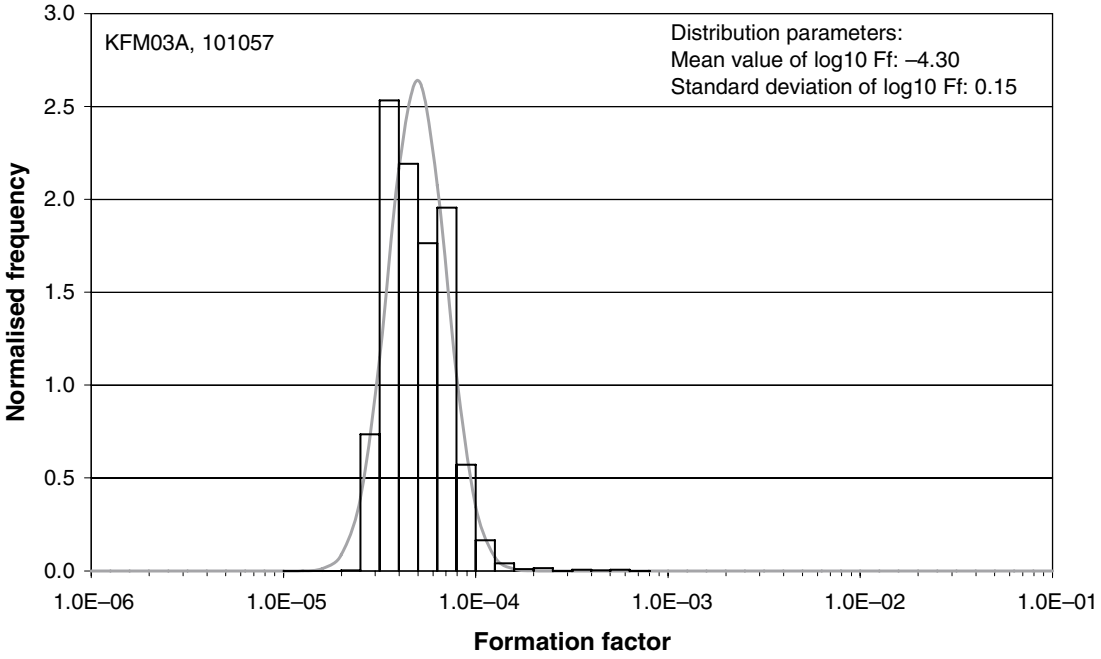

Rock type: 101057 = Granite to granodiorite, metamorphic, medium-grained
Length of core: 669 m (74%)
Number of data points: 2,921
Arithmetic mean: 5.32E–05

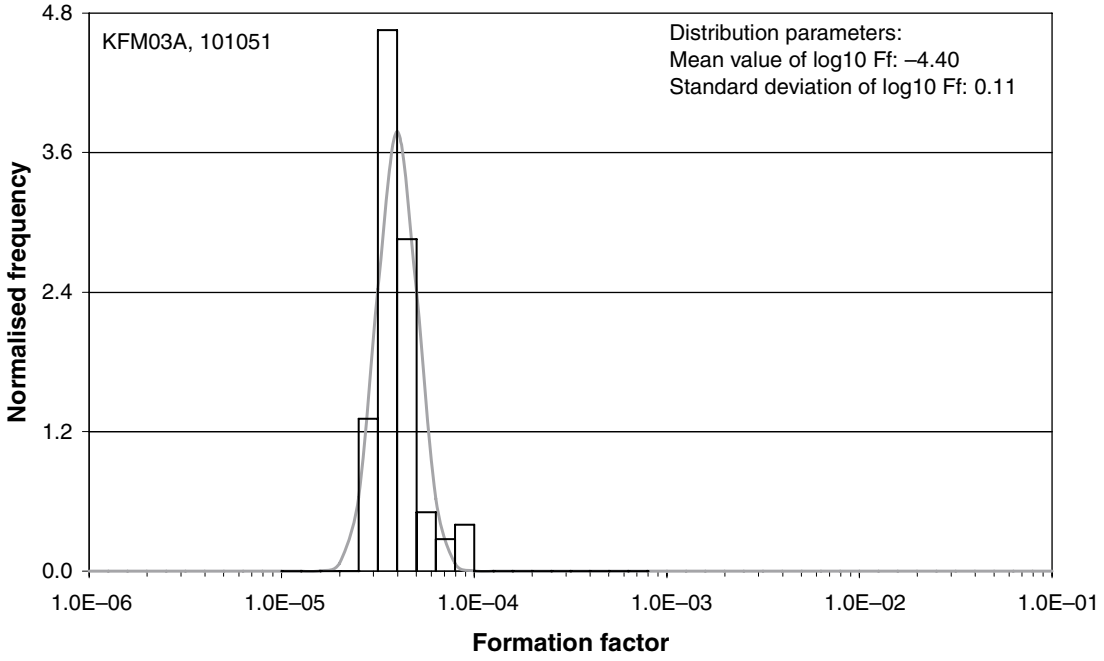

Rock type: 101051 = Granite, granodiorite and tonalite, metamorphic, fine- to medium-grained
Length of core: 118 m (13%)
Number of data points: 473
Arithmetic mean: 4.12E–05

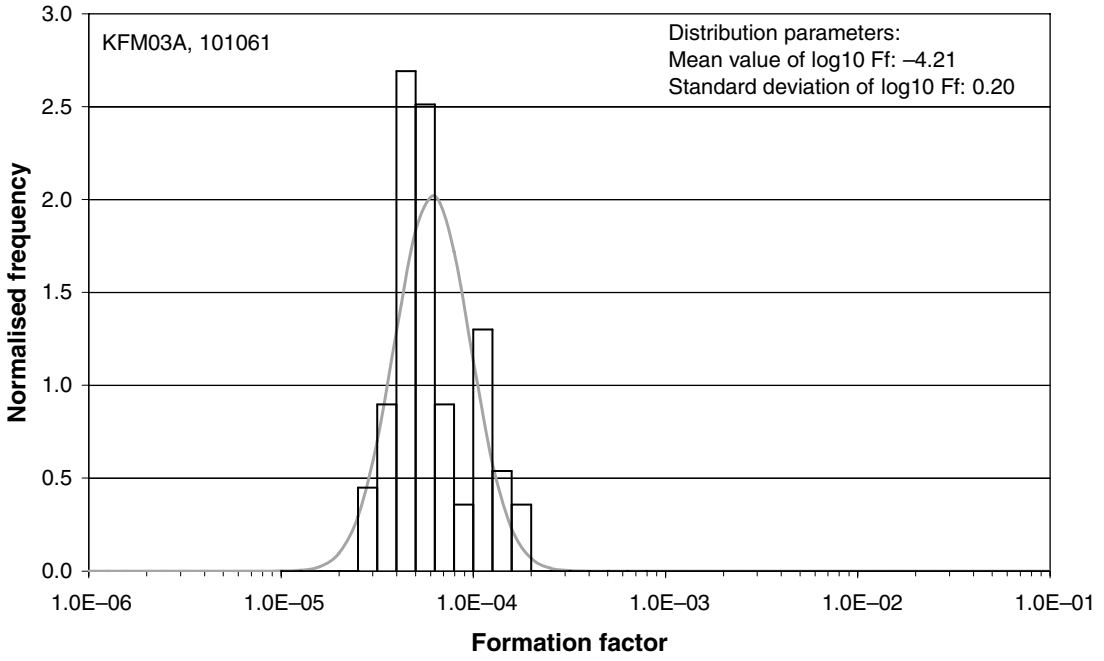

Rock type: 101061 = Pegmatite, pegmatitic granite
Length of core: 62 m (6.9%)
Number of data points: 223
Arithmetic mean: 6.88E–05

Appendix D2: Rock type specific distributions of fractured rock formation factors KFM03A

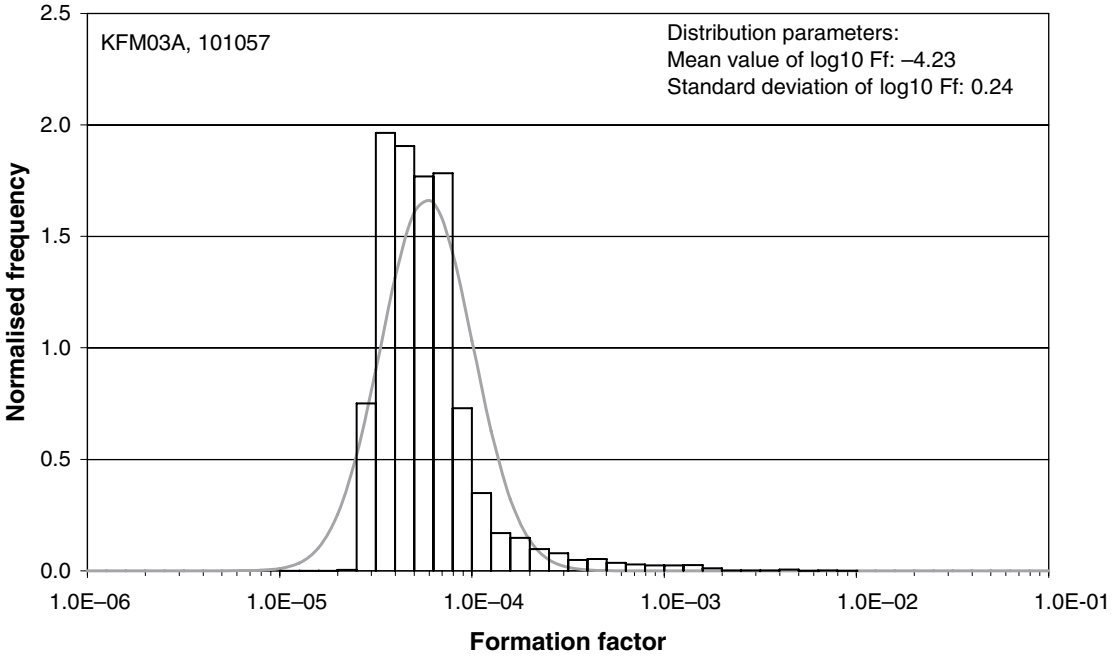

Rock type: 101057 = Granite to granodiorite, metamorphic, medium-grained
Length of core: 669 m (74%)
Number of data points: 5,622
Arithmetic mean: 8.28E–05

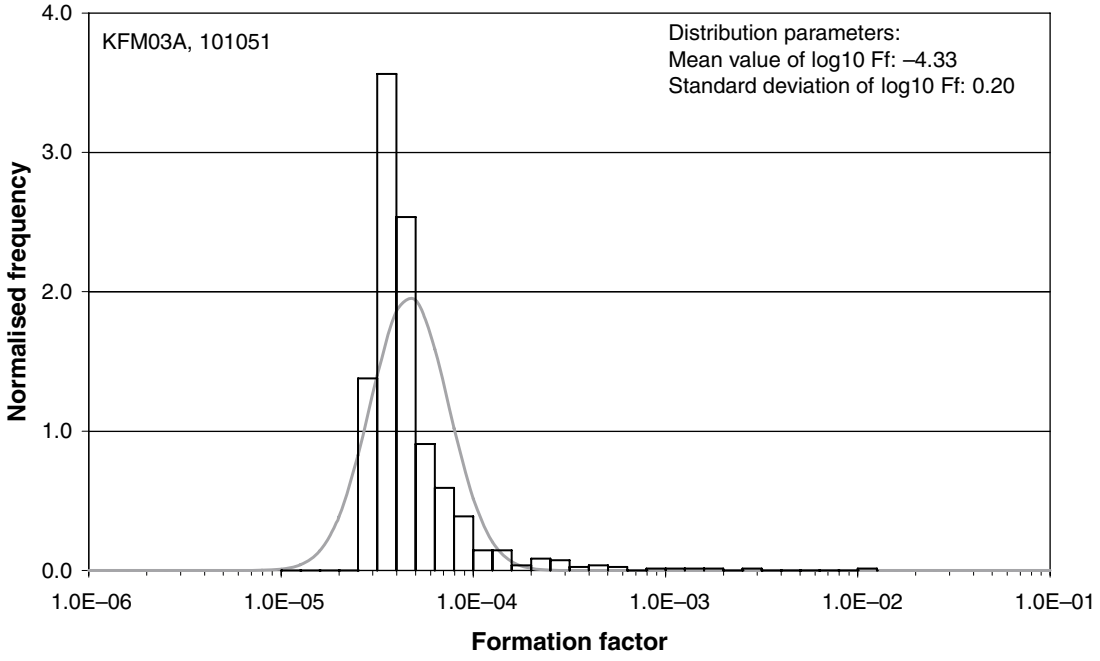

Rock type: 101051 = Granite, granodiorite and tonalite, metamorphic, fine- to medium-grained
Length of core: 118 m (13%)
Number of data points: 828
Arithmetic mean: 7.72E–05

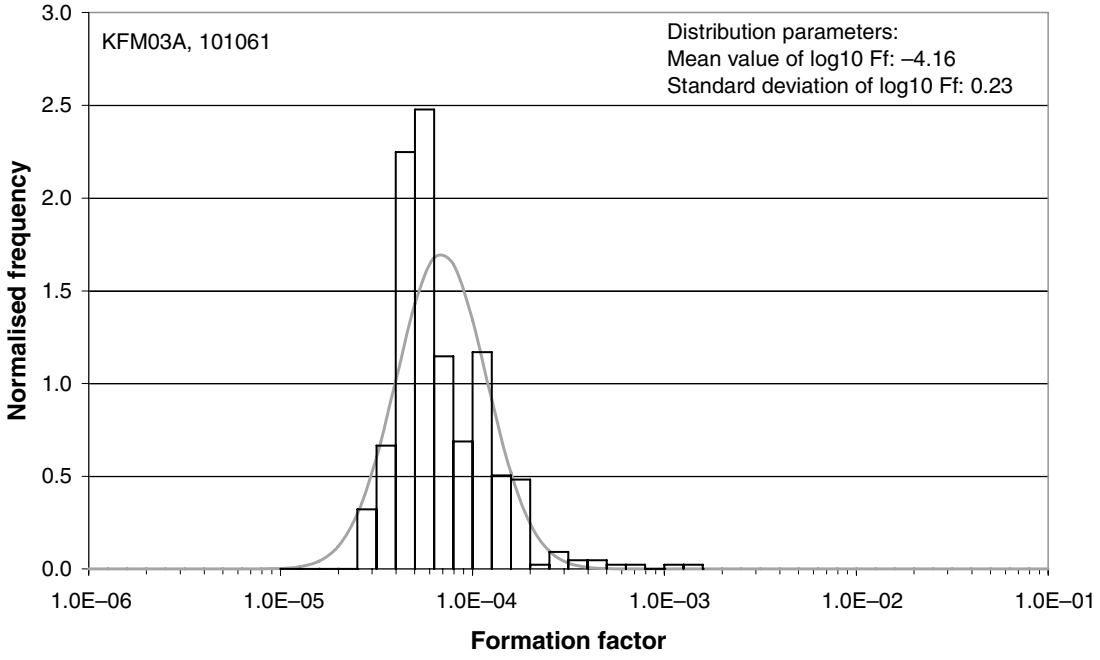

Rock type: 101061 = Pegmatite, pegmatitic granite
Length of core: 62 m (6.9%)
Number of data points: 436
Arithmetic mean: 8.63E–05

Appendix D3: Rock type specific distributions of rock matrix formation factors KFM04A

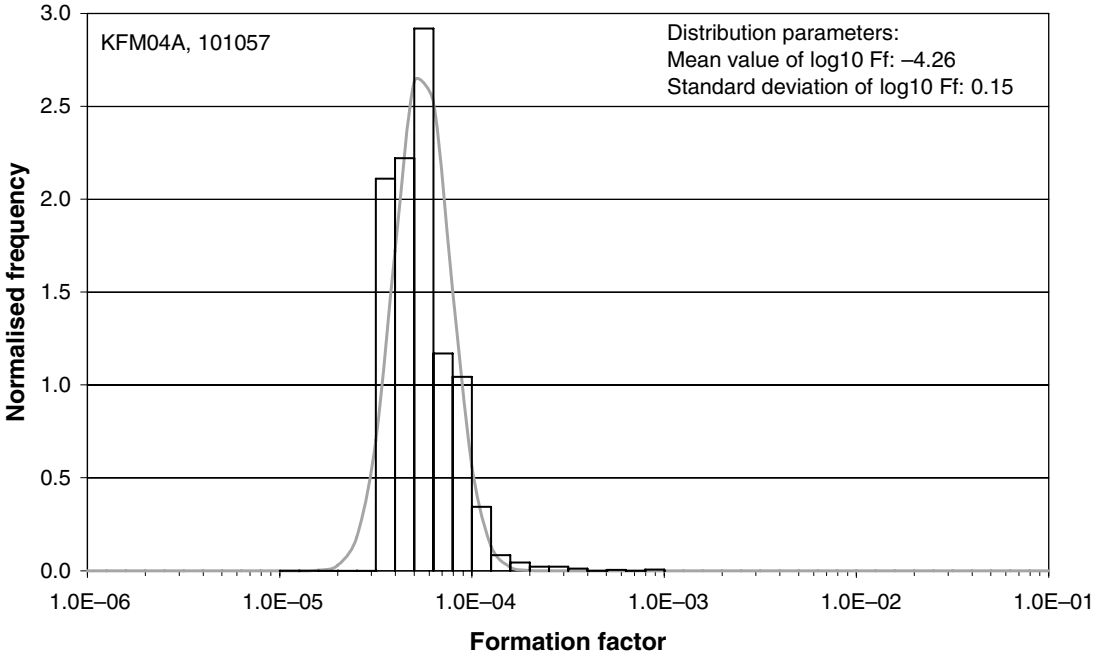

Rock type: 101057 = Granite to granodiorite, metamorphic, medium-grained
Length of core: 655 m (73%)
Number of data points: 2,711
Arithmetic mean: 5.95E–05

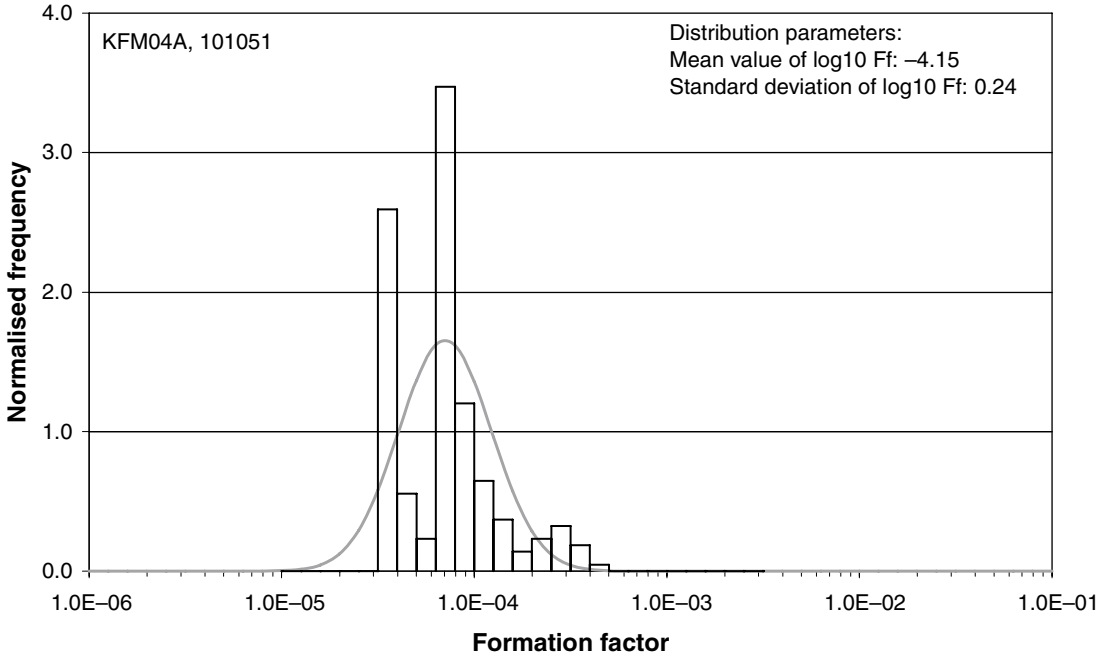

Rock type: 101051 = Granite, granodiorite and tonalite, metamorphic, fine- to medium-grained
Length of core: 103 m (12%)
Number of data points: 216
Arithmetic mean: 8.62E–05

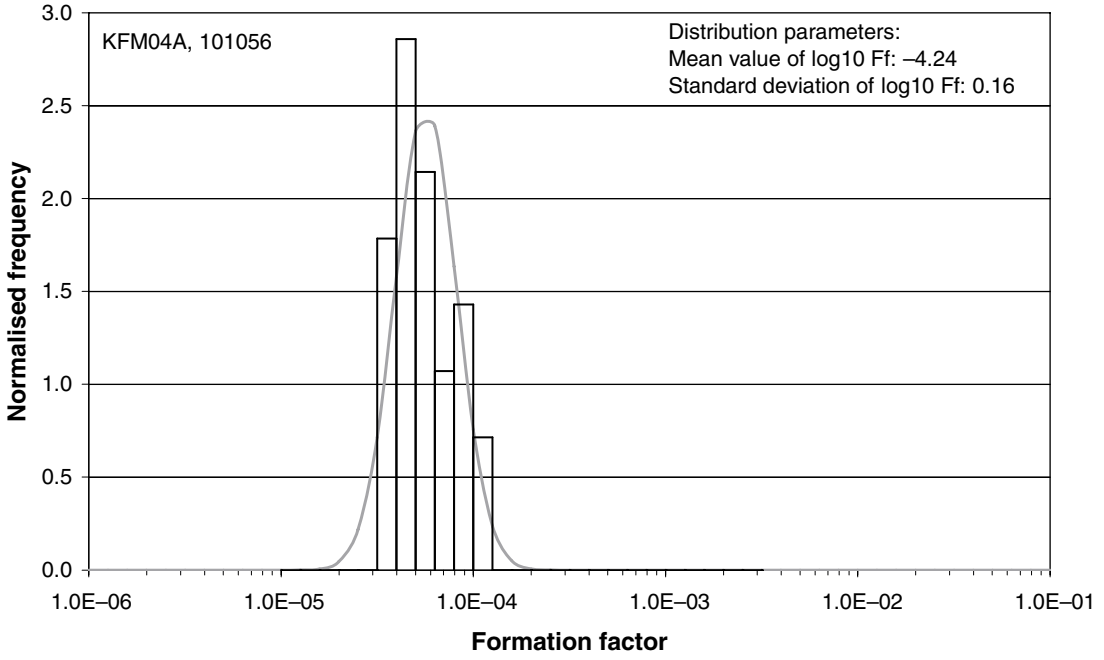

Rock type: 101056 = Granodiorite, metamorphic
Length of core: 65 m (7.3%)
Number of data points: 28
Arithmetic mean: 6.00E–05

Appendix D4: Rock type specific distributions of fractured rock formation factors KFM04A

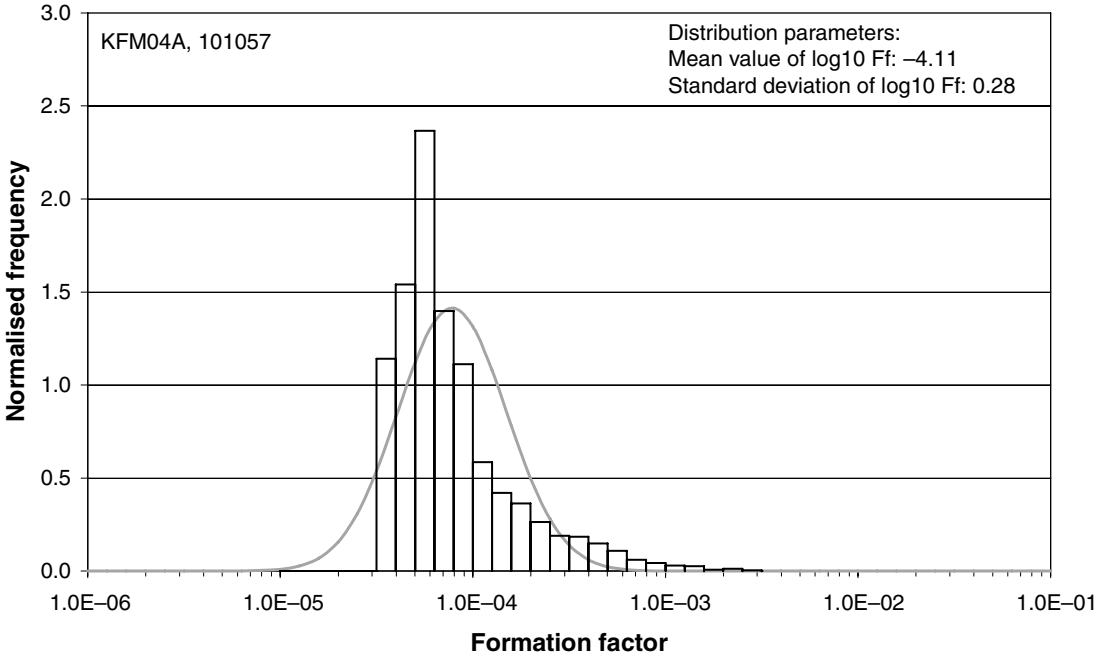

Rock type: 101057 = Granite to granodiorite, metamorphic, medium-grained
Length of core: 655 m (73%)
Number of data points: 6,416
Arithmetic mean: 1.13E–04

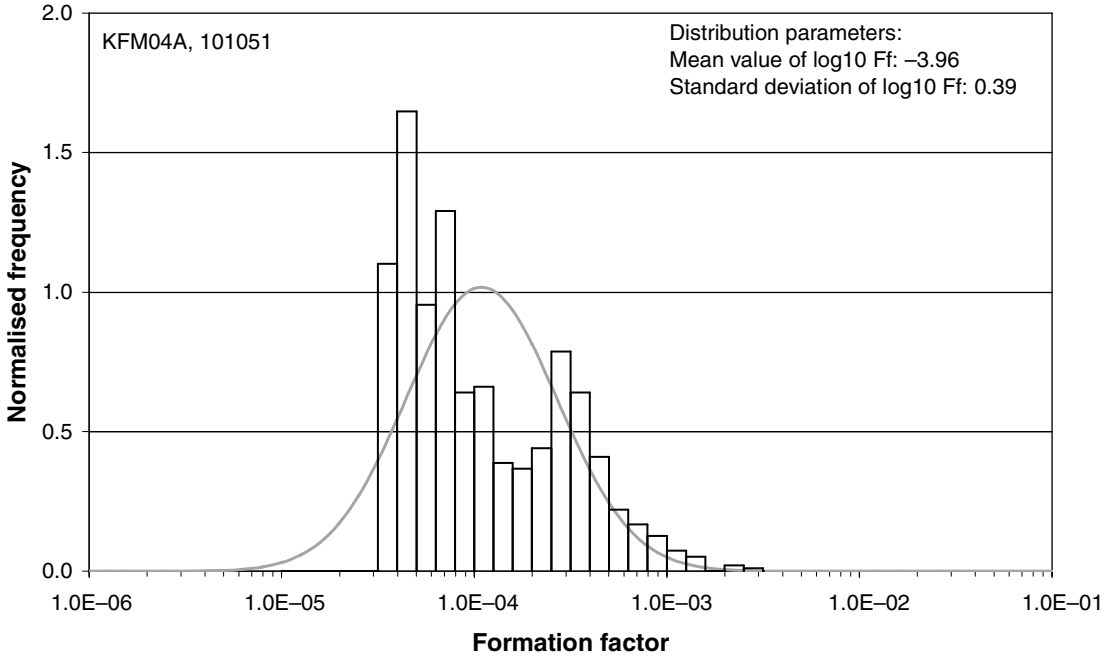

Rock type: 101051 = Granite, granodiorite and tonalite, metamorphic, fine- to medium-grained
Length of core: 103 m (12%)
Number of data points: 953
Arithmetic mean: 1.82E–04

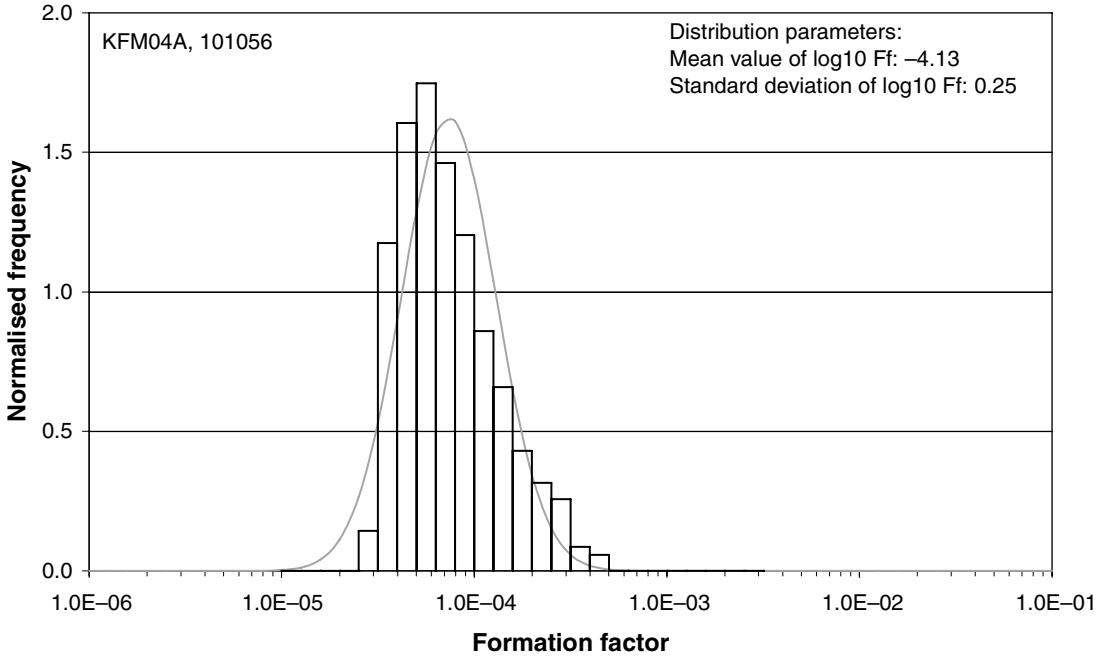

Rock type: 101056 = Granodiorite, metamorphic
Length of core: 65 m (7.3%)
Number of data points: 349
Arithmetic mean: 8.89E–05